



Importance of the vegetation-groundwater-stream continuum to understand transformation of biogenic carbon in aquatic systems – A case study based on a pine-maize comparison in a lowland sandy watershed (Landes de Gascogne, SW France)

Loris Deirmendjian ^{a,*}, Pierre Anschutz ^a, Christian Morel ^b, Alain Mollier ^b, Laurent Augusto ^b, Denis Loustau ^b, Luiz Carlos Cotovicz Jr ^{a,c}, Damien Buquet ^a, Katixa Lajaunie ^{a,d}, Gwenaëlle Chaillou ^e, Baptiste Voltz ^{a,f}, Céline Charbonnier ^a, Dominique Poirier ^a, Gwenaël Abril ^{a,c,g}

^a Laboratoire Environnements et Paléoenvironnements Océaniques et Continentaux (EPOC), CNRS, Université de Bordeaux, Allée Geoffroy Saint-Hilaire, 33615 Pessac Cedex, France

^b UMR 1391 ISPA, INRA, Bordeaux Sciences Agro, Villenave d'Ornon, 33883, France

^c Programa de pos-graduação em Geoquímica, Universidade Federal Fluminense, Outeiro São João Batista s/n, 24020015 Niterói, RJ, Brazil

^d Aix Marseille Université, CNRS/INSU, Université de Toulon, IRD, Mediterranean Institute of Oceanography (MIO) UM 110, France

^e Département Biologie, Chimie, Géographie, Université du Québec à Rimouski, Québec, Canada

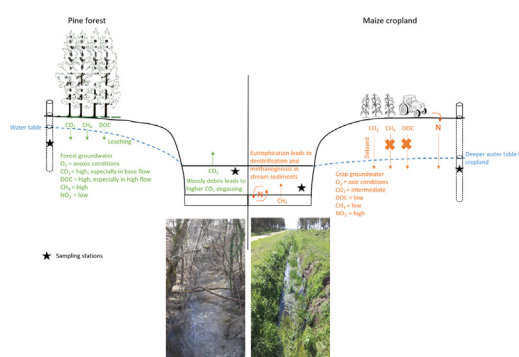
^f Univ. Lille, CNRS, Univ. Littoral Côte d'Opale, UMR 8187, LOG, Laboratoire d'Océanologie et de Géosciences, F 62 930 Wimereux, France

^g Biologie des Organismes et Ecosystèmes Aquatiques (BOREA), Muséum National d'Histoire Naturelle, CNRS, IRD, UPMC, UCBN, UAG. 61 rue Buffon, 75231 Paris cedex 05, France

HIGHLIGHTS

- Forest groundwater was in anoxic conditions whereas crop groundwater was in oxic conditions.
- Leaching of soil DOC occurred mostly in forest groundwater during high flow period.
- CO₂ and CH₄ were higher in forest groundwater than in crop groundwater.
- CH₄ was higher in crop streams compared to forest streams.
- CO₂ was not different between crop streams and forest streams.

GRAPHICAL ABSTRACT



ARTICLE INFO

Article history:

Received 14 October 2018

Received in revised form 19 December 2018

Accepted 13 January 2019

Available online 16 January 2019

José Virgílio Cruz

Keywords:

Carbon dioxide

Methane

ABSTRACT

During land-aquatic transfer, carbon (C) and inorganic nutrients (IN) are transformed in soils, groundwater, and at the groundwater-surface water interface as well as in stream channels and stream sediments. However, processes and factors controlling these transfers and transformations are not well constrained, particularly with respect to land use effect. We compared C and IN concentrations in shallow groundwater and first-order streams of a sandy lowland catchment dominated by two types of land use: pine forest and maize cropland. Contrary to forest groundwater, crop groundwater exhibited oxic conditions all-year round as a result of higher evapotranspiration and better lateral drainage that decreased the water table below the organic-rich soil horizon, prevented the leaching of soil-generated dissolved organic carbon (DOC) in groundwater, and thus limited consumption of dissolved oxygen (O₂). In crop groundwater, oxic conditions inhibited denitrification and methanogenesis resulting in high nitrate (NO₃⁻; on average

* Corresponding author at: Chemical Oceanography Unit, University of Liège, Liège, Belgium.

E-mail address: Loris.deirmendjian@uliege.be (L. Deirmendjian).

Groundwater
Stream
Land use
Pine
Maize

1140 ± 485 μmol L⁻¹) and low methane (CH₄; 40 ± 25 nmol L⁻¹) concentrations. Conversely, anoxic conditions in forest groundwater led to lower NO₃⁻ (25 ± 40 μmol L⁻¹) and higher CH₄ (1770 ± 1830 nmol L⁻¹) concentrations. The partial pressure of carbon dioxide (pCO₂; 30,650 ± 11,590 ppmv) in crop groundwater was significantly lower than in forest groundwater (50,630 ± 26,070 ppmv), and was apparently caused by the deeper water table delaying downward diffusion of soil CO₂ to the water table. In contrast, pCO₂ was not significantly different in crop (4480 ± 2680 ppmv) and forest (4900 ± 4500 ppmv) streams, suggesting faster degassing in forest streams resulting from greater water turbulence. Although NO₃⁻ concentrations indicated that denitrification occurred in riparian-forest groundwater, crop streams nevertheless exhibited important signs of spring and summer eutrophication such as the development of macrophytes. Stream eutrophication favored development of anaerobic conditions in crop stream sediments, as evidenced by increased ammonia (NH₄⁺) and CH₄ in stream waters and concomitant decreased in NO₃⁻ concentrations as a result of sediment denitrification. In crop streams, dredging and erosion of streambed sediments during winter sustained high concentration of particulate organic C, NH₄⁺ and CH₄. In forest streams, dissolved iron (Fe²⁺), NH₄⁺ and CH₄ were negatively correlated with O₂ reflecting the gradual oxygenation of stream water and associated oxidations of Fe²⁺, NH₄⁺ and CH₄. The results overall showed that forest groundwater behaved as source of CO₂ and CH₄ to streams, the intensity depending on the hydrological connectivity among soils, groundwater, and streams. CH₄ production was prevented in cropland in soils and groundwater, however crop groundwater acted as a source of CO₂ to streams (but less so than forest groundwater). Conversely, in streams, pCO₂ was not significantly affected by land use while CH₄ production was enhanced by cropland. At the catchment scale, this study found substantial biogeochemical heterogeneity in C and IN concentrations between forest and crop waters, demonstrating the importance of including the full vegetation-groundwater-stream continuum when estimating land-water fluxes of C (and nitrogen) and attempting to understand their spatial and temporal dynamics.

© 2019 Elsevier B.V. All rights reserved.

1. Introduction

Despite their small surface area worldwide (Downing et al., 2012), inland waters have been recognized as key component of the global carbon (C) cycle, constituting a preferential pathway of dissolved and particulate C transport from terrestrial ecosystems to the coastal ocean (Cole et al., 2007; Meybeck, 1982; Ludwig et al., 1996a, 1996b; Meybeck, 1987). Inland waters act as significant sources of carbon dioxide (CO₂) and methane (CH₄) to the atmosphere because inland waters are generally supersaturated by CO₂ and CH₄ compared to the overlying atmosphere (Abril et al., 2014; Bastviken et al., 2011; Borges et al., 2015; Lauerwald et al., 2015; Raymond et al., 2013; Stanley et al., 2016).

Inland waters and specifically small streams are tightly connected to their catchment characteristics such as hydrology and land use, as they receive large inputs of C from land (mainly from soils and groundwater), which in turn control the stream biogeochemical processes and the water composition (Aitkenhead et al., 1999; Deirmendjian and Abril, 2018; Hotchkiss et al., 2015; Johnson et al., 2006; Jones and Mulholland, 1998; McClain et al., 2003; Polsenare and Abril, 2012; Bodmer et al., 2016; Findlay et al., 2001; Lehrter, 2006). Groundwater discharge has been recognized as an important source of CO₂ in riverine systems, especially in small streams and headwaters (Deirmendjian and Abril, 2018; Hotchkiss et al., 2015; Johnson et al., 2008; Kokic et al., 2015; Marx et al., 2017; Raymond et al., 2013; Wallin et al., 2013). On the contrary to riverine CO₂, riverine CH₄ is likely to originate from wetlands that generally combine a strong hydrological connectivity with riverine waters and a high productivity (Abril et al., 2014; Abril and Borges, 2018). Although some studies found low CH₄ concentrations in the groundwater of Belgium (up to 1.1 μmol L⁻¹; Borges et al., 2018; Jurado et al., 2017), other studies found high CH₄ concentrations in the groundwater of Great Britain (up to 295 μmol L⁻¹; Bell et al., 2017) and in the Appalachian basin of the USA (up to 28,000 μmol L⁻¹; Molofsky et al., 2016). Actually, soil moisture, which controls oxic/anoxic conditions in soil, is the main determinant of terrestrial CO₂ or CH₄ production in soil. As a consequence, CH₄ emissions from soils are high under strictly anaerobic conditions in waterlogged soils whereas CO₂ emissions from soils are high under aerobic conditions in drier soils (Christensen et al., 2003; Moore and Knowles, 1989). Croplands affect water mass balance at the plot scale, especially through irrigation and extraction of groundwater, which results in declining water

table in many regions worldwide (Foley et al., 2005; Gleick, 2003; Jackson et al., 2001; Postel, 1999; Rosegrant et al., 2002). Investigating spatial dynamics of CO₂ and CH₄ in groundwater in relation with land use is critical better understanding processes governing their terrestrial production and leaching to groundwater.

Croplands cover about 40% of the terrestrial ice-free surface and are often associated with degradation of both ground and surface water quality (Asner et al., 2004; Clague et al., 2015; Foley et al., 2005; Hiscock et al., 1991; Ramankutty and Foley, 1999). Intensive agriculture led to an increase of nitrate (NO₃⁻) entering ground and surface water environments that has fueled aquatic primary production in surface waters and led to low CO₂ and high CH₄ concentrations, the latter being related to enhanced organic matter delivery in sediments (Borges et al., 2018; Carpenter et al., 1998; Clague et al., 2015; Crawford et al., 2016; Jordan and Weller, 1996; Smith, 2003; Zhou et al., 2017). Additionally, aquatic primary production in crop streams is enhanced as a result of low light limitation (clearing of riparian vegetation), and the excessive transport of sediment-bound organic matter and nutrients to surface waters (Bernot et al., 2010; Lamba et al., 2015; Ramos et al., 2015; Young and Huryn, 1999). Soil erosion rates in agricultural landscapes are one to two times larger than those in areas with native vegetation (Montgomery, 2007; Quinton et al., 2010). Indeed, riparian forest is usually considered stream buffer zones that attenuate stream bank erosion and NO₃⁻ inputs from croplands (Balestrini et al., 2016; Cey et al., 1999; Christensen et al., 2013; Stott, 2005; Wynn and Mostaghimi, 2006). Denitrification represents a permanent removal pathway that limits the extent and impact of NO₃⁻ contamination by transforming NO₃⁻ to inert dinitrogen (N₂). However, incomplete denitrification can produce nitrous oxide (N₂O), a major anthropogenic ozone-depleting substance (Ravishankara et al., 2009). On the contrary to croplands, forests are known to export fewer nutrients by limiting runoff and leakage of nutrients (Canton et al., 2012; Onderka et al., 2010).

Land use effects on both water composition and biogeochemical processes have been studied in streams and groundwater (Barnes and Raymond, 2010, 2009; Bernot et al., 2010; Bodmer et al., 2016; Jeong, 2001; Lehrter, 2006; Masese et al., 2017; Raymond and Cole, 2003; Rodrigues et al., 2018; Salvia-Castellví et al., 2005; Vidon et al., 2008; Wilson and Xenopoulos, 2009; Young and Huryn, 1999; Zhang et al., 2018), but land use studies with simultaneous groundwater and stream sampling are more scarce (Bass et al., 2014; Borges et al., 2018; Hu et al.,

2016). The objective of this study was to understand how two contrasting types of land use (pine forest and maize cropland) affected C and inorganic nutrient (IN) concentrations in shallow groundwater and in first-order streams of a sandy lowland catchment. We hypothesized that the biogeochemical variability between crop groundwater and forest groundwater was due to agricultural practices that affect N inputs (fertilizer) and water mass balance (irrigation and drainage). We hypothesized that the biogeochemical variability between crop and forest streams originate from differential lateral export of C and IN from two distinct sources (i.e., crop groundwater and forest groundwater) because of a strong hydrological connection between groundwater and streams in the studied catchment.

2. Materials and methods

2.1. Study site

The Leyre catchment (2100 km²) is located in the southwestern part of France. This is a flat coastal plain with a mean slope lower than 0.125% and a mean altitude lower than 50 m (Jolivet et al., 2007). The lithology is relatively homogeneous and composed of sandy permeable surface layers dating from the Plio-Quaternary period (Legigan, 1979; Bertran et al., 2009, 2011). The soils are podzols characterized by a low pH (≈ 4), low nutrient availability, low cationic exchange capacity, and high organic C content that can reach 50 g per kg of soil (Augusto et al., 2010; Lundström et al., 2000). In Leyre sandy podzols, the low clay and silt content causes a low soil water retention (Augusto et al., 2010).

The study area was a vast wetland until the 19th century, when a wide forest of maritime pine was sown following a landscape drainage campaign resulting from an imperial decree of Napoleon III in 1857 (Jolivet et al., 2007). Currently, the catchment is mainly occupied by C₃ pine forest (approximately 85%), with a modest proportion of C₄ maize cropland (approximately 15%) (Fig. 1; Jolivet et al., 2007). Following catastrophic forest wildfires, the maize croplands were installed

during the second half of the 20th century. Consequently, their spatial distribution was not based on soil properties, as confirmed by the similar mean values of soil texture in local croplands and forests (Augusto et al., 2010; Jolivet et al., 2003). During the maize cropping season (usually May to November), farmers irrigate the plots by pumping shallow groundwater (~ 1 –5 m deep) almost daily to maintain adequate soil moisture status, whereas maritime pine stands are never irrigated (Govind et al., 2012). As N is not limiting for tree growth in our study region (Trichet et al., 2009), forests are never fertilized with N. Conversely, croplands generally receive two N fertilizer applications annually, a first at the beginning of May (30–50 kg N ha⁻¹), and second at the beginning of June with 200–250 kg N ha⁻¹ (Canton et al., 2012; Jambert et al., 1997; Ulrich et al., 2002). Additionally, in order to maintain soil pH in the 5.5–6.0 range, local maize croplands are limed with crushed limestone (CaCO₃) containing a small portion of dolomite (CaMg(CO₃)₂) (10 t ha⁻¹ right after forest conversion and then 0.5 t ha⁻¹ an⁻¹; Jolivet et al., 2003).

The climate is oceanic with a mean annual air temperature of 13 °C and a mean annual precipitation of 930 mm (Moreaux et al., 2011). Owing to the low slope, the low soil water retention and the high permeability of the soil (i.e., hydraulic conductivity is approximately 40 cm h⁻¹, Corbier et al., 2010), the percolation of rain water is fast (55 cm h⁻¹ on average, Vernier and Castro, 2010). Consequently, surface runoff does not occur as the excess of rainfall percolates into the soil and recharges the shallow groundwater, causing the water table to rise. The sandy permeable surface layers contain a free and continuous water table that is strongly interconnected with the superficial river network. This is facilitated by a dense network of drainage ditches, initiated in the 19th century and currently maintained by forest managers in order to enhance tree regeneration and growth (Thivolle-Cazat and Najar, 2001). During the sampling period, channels of some crop streams were dredged before they began to flow again. This was done to optimize local cropland drainage and to feed croplands with IN and organic residuals found in the stream sediments. To increase soil permeability and to optimize lateral drainage in local maize

Legend

- Leyre catchment
- Forest streams
- Crop streams
- ▲ Riparian groundwater
- Crop groundwater
- Forest groundwater
- Main stems
- River network
- Urban
- Cropland
- Forest

N

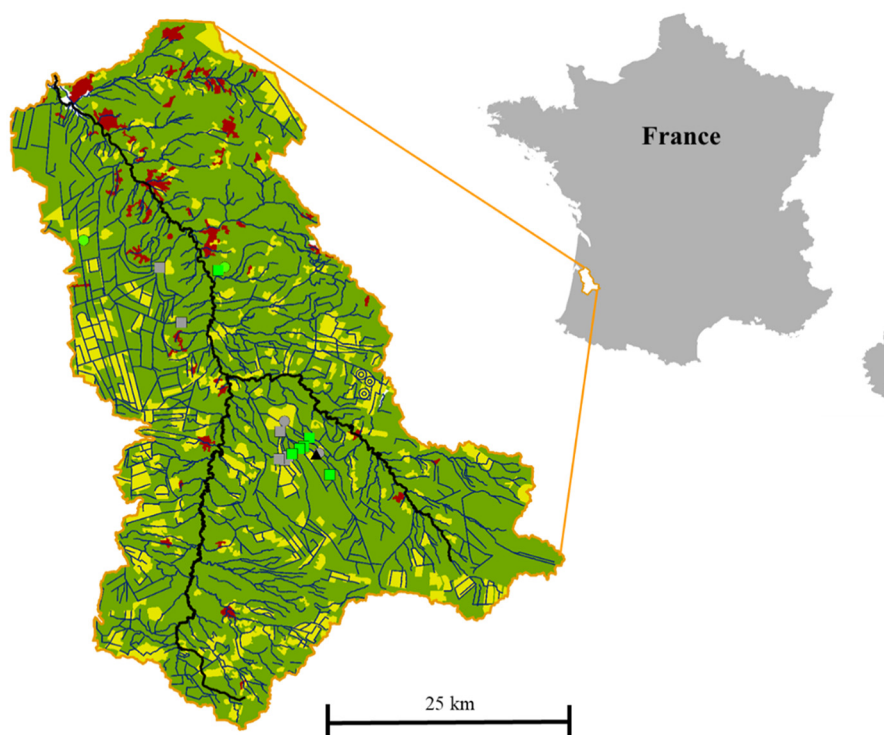


Fig. 1. Land use map of the Leyre catchment showing river network and the sampling locations of groundwaters and streams.

croplands, farmers practice subsoiling and agricultural ditches are generally deeper (2.0–2.5 m) than forest ditches (1.0 m).

2.2. Sampling strategy

We defined order 0 as groundwater and order 1 as streams and ditches either having no tributaries or being seasonally dry (from June to December during our sampling period). We selected 17 sampling stations (5 shallow groundwater and 12 first-order streams) within the Leyre catchment (Table 1; Fig. 1). The groundwater sampling stations were located in maize cropland ($n = 2$), pine forest ($n = 2$; one is the Bilos station (FR-Bil) of the ICOS Research infrastructure) and in a riparian forest adjacent to a maize cropland ($n = 1$; Table 1; Fig. 1). The stream sampling stations were chosen based on the different proportions of croplands in their respective catchments (Table 1; Fig. 1).

Groundwater was sampled for temperature, electrical conductivity (EC), pH, dissolved oxygen (O_2), methane (CH_4), partial pressure of CO_2 (pCO_2), total alkalinity (TA), dissolved inorganic carbon (DIC), stable isotope composition of the dissolved inorganic carbon ($\delta^{13}C$ -DIC), dissolved organic carbon (DOC), ammonia (NH_4^+), nitrate (NO_3^-) and dissolved iron (Fe^{2+}). For groundwater, we took the precaution to renew the water in the piezometers by pumping with a submersible pump before sampling. Groundwater was then sampled once the stabilization (approximately 10 min) of groundwater temperature, pH, EC and O_2 monitored with portable probes was observed. Streams were sampled for the same parameters, plus total suspended matter (TSM), particulate organic carbon (POC) and the POC content of the TSM (POC%).

2.3. Field measurements and laboratory analyses

Groundwater and streams were sampled at approximately monthly time intervals between Jan. 2014 and Jul. 2015 (Table S1). In total, throughout the sampling period, we sampled 55 groundwaters and 137 stream waters.

The pCO_2 in groundwater and streams was measured directly using an equilibrator (Frankignoulle and Borges, 2001; Polsenaere et al., 2013) following the procedure of Deirmendjian and Abril (2018).

We stored the total alkalinity (TA) samples in polypropylene bottles after filtration using a syringe equipped with glass fiber filters (GF/F; $0.7 \mu m$). TA was then analyzed on filtered samples by automated electro-titration on 50 mL samples with 0.1 N HCl as the titrant. The equivalence point was determined from pH between 4 and 3 with the Gran method (Gran, 1952). Precision based on replicate analyses was better than $\pm 5 \mu mol L^{-1}$. For samples with a very low pH (< 4.5), we bubbled the water with atmospheric air in order to degas the CO_2 . Consequently, the initial pH increased above 5, and the TA titration was then performed (Abril et al., 2015).

We calculated DIC from pCO_2 , TA, and temperature measurements using the carbonic acid dissociation constants of Millero (1979) and the CO_2 solubility from Weiss (1974), using the CO_2SYS software (Lewis et al., 1998). The $\delta^{13}C$ -DIC samples were collected using 120 mL glass serum bottles sealed with a rubber stopper and treated with 0.3 mL of $HgCl_2$ at $20 g L^{-1}$ to avoid any microbial respiration during storage. Vials were carefully sealed such that no air remained in contact with samples and were stored in the dark to prevent photo-oxidation. The $\delta^{13}C$ -DIC measurements were performed with the headspace technique using an isotope ratio mass spectrometer coupled to an elemental analyzer (EA-IRMS, Micromass IsoPrime) equipped with a manual gas injection port as described in Gillikin and Bouillon (2007).

CH_4 was also measured using a headspace technique in 60 mL glass serum bottles. The headspace was created with 10 mL of N_2 gas. We then injected 0.5 mL of the headspace in a gas chromatograph equipped with a flame ionization detector (GC-FID).

DOC samples were obtained after filtration in the field through pre-combusted GF/F ($0.7 \mu m$). DOC filtrates were stored in pre-combusted Pyrex vials (25 mL), acidified with 50 μL of 37% HCl to reach pH 2, and kept at $4^\circ C$ in the laboratory before analysis. The DOC concentrations were measured with a SHIMADZU TOC 500 analyzer (in TOC-IC mode), using a technique based on thermal oxidation after a DIC removal step (Sharp, 1993). The repeatability was better than $10 \mu mol L^{-1}$.

Table 1
Characteristics of groundwater and stream sampling stations, ranked in decreasing order of cropland percentage in their respective sub-catchments. ^a delimited with a geographic information system software (ArcGIS 10.5®) using an hydrological database in a polyline form (BD CARTHAGE®) and a digital elevation model (BD ALTI®, resolution of 25 m), which both have been made available by the national geographic institute of France (<http://www.ign.fr/>). ^b retrieved with the CORINE land cover 2006 database (EEA, 2014) using a geographic information system software (ArcGIS 10.5®). ^c C, F, R corresponding to crop, forest and riparian waters, respectively, either during high or base flow. Piezometer 1 (P1) is located in a riparian mixed pine and oak forest near a first-order stream and near a maize cropland, which where P2 is located. P2 and P3 are located in the middle of two different maize croplands of 0.6 km² and 6 km², respectively. P5 is located in an 11-years old pine plot of 0.6 km² and is part of the ICOS (name is FR-Bil) research infrastructure (<http://icos-ri.eu>), whereas P4 is located in another pine forest (approximately same age as P5 pine forest). The depth of piezometers (from the soil surface to the bottom of the piezometer) is 5.3 m for P1, 4.9 m for P2, 9.1 m for P3, 5 m for P4 and P5.

Stream order	Description	Catchment area (km ²) ^a	Crop (%) ^b	Forest (%) ^b	Urban (%) ^b	During high flow ^c	During base flow ^c
1	Ditch	1.0	86.5	13.5	0.0	C	C
1	Ditch	1.3	53.8	46.2	0.0	C	C
1	Ditch	11.3	44.2	55.8	0.0	C	C
1	Ditch	13.4	42.5	57.5	0.0	C	C
1	Stream	57.0	30.7	69.3	0.0	C	C
1	Stream	16.8	7.8	92.2	0.0	F	F
1	Ditch	7.9	5.8	94.2	0.0	F	F
1	Ditch	2.3	5.2	94.8	0.0	F	C
1	Stream	16.0	4.6	93.8	1.6	C	F
1	Stream	34.0	3.8	96.2	0.0	F	F
1	Stream	31.0	2.3	97.7	0.0	F	F
1	Headwater	0.3	0.0	100.0	0.0	F	F
0	Groundwater in a riparian forest but very near (5 m) a maize cropland (P1)					R	R
0	Groundwater in maize cropland (P2)					C	C
0	Groundwater in maize cropland (P3)					C	C
0	Groundwater in pine forest (P4)					F	F
0	Groundwater in pine forest (P5)					F	F

The water for TSM and POC measurements was filtered through pre-weighed and pre-combusted GF/F glass fiber filters (0.7 μm). The filters were dried at 60 °C and stored in the dark, and subsequently, TSM was determined by gravimetry. POC was measured using the same filter. The filters were acidified in crucibles with 2 N HCl to remove carbonates and were then dried at 60 °C to remove inorganic carbon and most of the remaining acid and water (Etcheber et al., 2007). POC content was measured by combustion (1500 °C) using a LECO CS 200 analyzer and the CO_2 formed was determined quantitatively by infrared absorption. POC in $\mu\text{mol L}^{-1}$ and POC% were then calculated. The uncertainty was $\pm 0.05\%$ of TSM.

For IN determination, water was filtered through a 0.20 μm cellulose acetate syringe membrane. Subsamples for Fe^{2+} were acidified with 37% HCl to prevent precipitation of iron oxide, whereas subsamples for NH_4^+ and NO_3^- were not acidified but kept frozen until later analyses. Then, NH_4^+ , NO_3^- , and Fe^{2+} were analyzed by colorimetry according to standard techniques. NH_4^+ was analyzed following the procedure of Harwood and Kühn (1970). NO_3^- was analyzed by flow injection analysis following the procedure of Anderson (1979). Fe^{2+} was analyzed using the ferrozine method (Stookey, 1970). Precision was $\pm 10\%$ for NH_4^+ and NO_3^- , and was $\pm 5\%$ for Fe^{2+} .

EC, temperature, O_2 , and pH were measured using portable probes (WTW®). Before each field trip, the pH probe was calibrated using two NBS buffer solutions (4 and 7), the oxygen polarographic probe was calibrated to 100% in a humid atmosphere and the conductivity probe was calibrated using a salinity standard.

2.4. Statistical analyses

K-means clustering analysis (MacQueen, 1967) was used to classify waters either as forest-dominated or as cropland-affected (Table 1). Indeed, K-means clustering analysis allows partitioning a dataset into k groups (i.e., clusters) pre-specified by the analyst (MacQueen, 1967). Contrary to forest waters at our study site, crop waters exhibit disproportionately higher NO_3^- concentration as a result of N fertilizer use on maize cropland (Canton et al., 2012; De Wit et al., 2005; Jambert et al., 1997, 1994). Consequently, in the K-means clustering analysis we used NO_3^- concentration data as a proxy to establish a statistical distinction between forest and crop waters (Table 1). K-means clustering analysis was performed one time with the groundwater dataset (but excluding the riparian groundwater) and a second time with the first-order streams dataset. We excluded data from riparian groundwater because we have considered riparian groundwater as a cluster itself (Table 1).

Principal component analysis (PCA) was used to condense multivariate information on correlated biogeochemical parameters to a set of uncorrelated variables called principal components (further referred to as dimensions). PCA was performed one time with a dataset consisting of each measured parameter in groundwater (but excluding the riparian groundwater) and a second time with the corresponding first-order streams dataset. PCA was performed separately for groundwater and streams because particulate parameters were not present in groundwater. If PCA were not performed separately for groundwater and streams, all data from groundwater would have been removed from the analysis (indeed, if one parameter is missing for a given sampling station, the sampling station is entirely deleted from the PCA). In addition, performing the PCA separately for groundwater and streams led to information that was more robust with respect to the biogeochemical variability induced by land use, in either groundwater or streams. However, to observe whether the two groundwater (crop and forest) and two streams (crop and forest) sources could be distinguished mathematically in one PCA, we performed an additional PCA with data from both groundwater and streams that excluded particulate parameters from the analysis. All concentrations data were log-transformed prior to PCA. The PCAs showed the biogeochemical

variability across forest, cropland, and hydrological seasons in either groundwater or first-order streams.

Later, non-parametric bivariate analyses (Mann-Whitney statistical tests) were used to estimate if hydrological seasons or increasing stream order significantly influenced the concentration of a biogeochemical parameter. Linear regressions were performed to model the relationships between two variables by fitting a linear equation to observed data.

K-means clustering analysis (package Stats) and PCA analysis (package FactoMineR for analysis and package factoextra for visualization; Kassambra and Mundt, 2017; Lê et al., 2008) were performed with R software version 3.1.4 (R Core Team, 2018). Mann-Whitney tests and linear regressions were performed with Graph Pad Prism version 7 software.

3. Results

3.1. Hydrology

In previous work based on the same dataset, but excluding cropland sampling stations, we identified two major hydrological seasons (Deirmendjian and Abril, 2018). One defined a high flow period as two relatively short flood events that occurred in Jan. 2014–Mar. 2014 and in Feb. 2015–Mar. 2015, whereas we defined the base flow period as two longer periods of low flow occurring in Apr. 2014–Jan. 2015 and Apr. 2015–Jul. 2015. During high flow, the average and the maximum river flows were $50 \text{ m}^3 \text{ s}^{-1}$ and $119 \text{ m}^3 \text{ s}^{-1}$, respectively. During base flow, the average and the minimum river flow were $10 \text{ m}^3 \text{ s}^{-1}$ and $5 \text{ m}^3 \text{ s}^{-1}$, respectively. The water tables in the forest, riparian forest, and cropland exhibited similar temporal fluctuations but with a different intensity, and the forest had an overall higher water table depth than the cropland (Fig. 2). The water table in the riparian area exhibited intermediate depth between the forest and cropland sites (Fig. 2). As surface runoff was negligible in the studied sandy and flat catchment, most of the stream water likely originated from groundwater discharge.

To investigate the temporal variability of the studied biogeochemical parameters, we chose to rely on hydrological regimes (high flow and base flow periods) rather than on temperature periods (seasons). At our study site climate was oceanic (by definition very temperate) and the amplitude of the water temperature was not as high as the amplitude of the river flow. As an example, Leyre River (main stem) flow could be up to $119 \text{ m}^3 \text{ s}^{-1}$ and could be down to $5 \text{ m}^3 \text{ s}^{-1}$, whereas the highest water temperature amplitude occurred in forest streams and was 6.4–25.8 °C (Table 2). Additionally, most of the lateral export

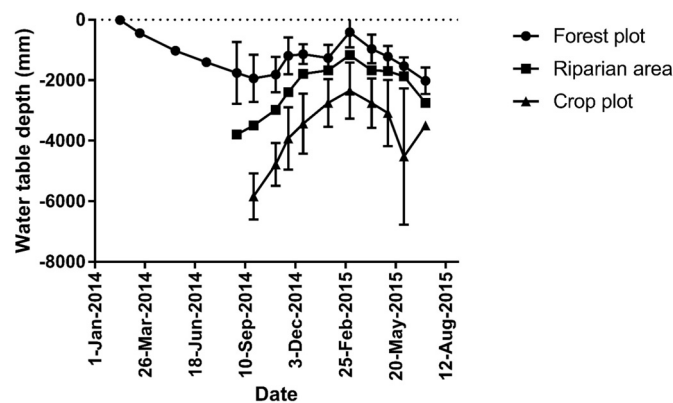


Fig. 2. Water table depth during the sampling period (Jan. 2014–Jul. 2015) across land use in the Leyre catchment. The water table in riparian area is the water table at P1 (Table 1). The water table in crop plot is the average \pm standard deviations of water tables at P2 and P3 (Table 1). The water table in forest plot is the average \pm standard deviations of water tables at P4 and P5 (Table 1).

Table 2
Values of carbon and ancillary parameters throughout sampling period (Jan. 2014–Jul. 2015) in crop and forest continuums and in riparian groundwater. Numbers between brackets are corresponding to the sampling size. For each parameter, the table showed average \pm standard deviations and the range.

	Crop continuum		Forest continuum		Riparian groundwater
	Groundwaters (22)	Streams (59)	Groundwaters (22)	Streams (78)	Groundwaters (11)
pH	4.5 \pm 0.2 4.3–5.0	6.0 \pm 0.3 5.4–7.0	4.5 \pm 0.3 3.7–4.8	5.8 \pm 0.5 4.2–6.9	4.7 \pm 0.1 4.4–4.8
Temperature ($^{\circ}$ C)	14.5 \pm 1.8 10.7–17.5	13.6 \pm 4.2 6.4–25.8	12.8 \pm 1.8 8.5–15.1	12.9 \pm 3.9 4.8–22.1	14.9 \pm 2.4 11.8–17.9
EC (μ S cm $^{-1}$)	360 \pm 70 220–465	220 \pm 55 75–370	90 \pm 10 65–115	115 \pm 30 70–200	160 \pm 50 95–270
NO $_3^-$ (μ mol L $^{-1}$)	1140 \pm 485 260–1785	340 \pm 200 10–950	25 \pm 40 0–120	75 \pm 70 0–275	310 \pm 260 40–860
NH $_4^+$ (μ mol L $^{-1}$)	0.4 \pm 0.8 0–3.5	6.1 \pm 7.0 0–40	4.5 \pm 7.0 0.3–30	1.8 \pm 1.7 0–7.8	0.4 \pm 0.4 0–1.5
Fe $^{2+}$ (μ mol L $^{-1}$)	0.9 \pm 0.4 0.1–1.9	5.9 \pm 4.4 0.1–22	15 \pm 15 0.9 \pm 56	7.9 \pm 12.0 0.6 \pm 58	0.6 \pm 0.5 0.2–1.5
O $_2$ (μ mol L $^{-1}$)	220 \pm 65 100–315	290 \pm 45 160–400	20 \pm 30 0–110	280 \pm 50 110–370	100 \pm 70 0–170
CH $_4$ (nmol L $^{-1}$)	40 \pm 25 15–130	460 \pm 950 20–4900	1770 \pm 1830 50–6700	240 \pm 300 20–2370	1470 \pm 1490 30–4150
pCO $_2$ (ppmv)	30,650 \pm 11,590 19,000–60,550	4480 \pm 2680 1040–14,080	50,630 \pm 26,070 7680–116,380	4900 \pm 4500 1000–27,200	42,950 \pm 28,560 17,300–103,300
TA (μ mol L $^{-1}$)	90 \pm 25 35–130	100 \pm 50 30–300	70 \pm 30 30–135	90 \pm 50 30–280	70 \pm 15 45–85
δ^{13} C-DIC (‰)	–19.8 \pm 1.3 –22 to –17.6	–18.2 \pm 3.5 –27.6 to –11.3	–26.7 \pm 1.0 –28.8 to –24	–19.8 \pm 2.8 –27.6 to –14	–25.2 \pm 1.1 –27.9 to –23.4
DIC (μ mol L $^{-1}$)	1450 \pm 480 820–2590	315 \pm 135 90–650	2460 \pm 1130 570–5370	320 \pm 210 120–1280	1960 \pm 1150 940–4480
DOC (μ mol L $^{-1}$)	510 \pm 150 275–880	605 \pm 320 220–2290	930 \pm 930 310–3670	470 \pm 250 190–1725	400 \pm 100 280–620
TSM (mg L $^{-1}$)		5.6 \pm 8.6 0.1–50.5		2.3 \pm 1.7 0.4–8.2	
POC (%)		28 \pm 10 0–50		28 \pm 10 10–80	
POC (μ mol L $^{-1}$)		120 \pm 180 0–1100		50 \pm 35 0–170	

occurred during the short periods of high flow (up to 90% for DOC, Deirmendjian et al., 2018). Thus, characterizing biogeochemical variability and biogeochemical processes in relation with land use during

this hydrological period was important. Furthermore, the seasonality induced by water temperature was to a certain extent included in the defined hydrological regimes since the high flow period was associated

Table 3
Values of carbon and ancillary parameters throughout sampling period (Jan. 2014–Jul. 2015) in different types of groundwater across hydrological seasons. Numbers between brackets are corresponding to the sampling size. For each parameter, the table showed the average \pm standard deviations and the range. We defined six groups that are Cropland_HF/Cropland_BF, Forest_HF/Forest_BF and Riparian_HF/Riparian_BF corresponding to groundwaters during high flow (HF) or base flow (BF); in either cropland, forest or riparian forest.

	Groundwater					
	Cropland_HF (4)	Cropland_BF (18)	Forest_HF (6)	Forest_BF (16)	Riparian_HF (2)	Riparian_BF (9)
pH	4.6 \pm 0.3 4.3–4.9	4.5 \pm 0.2 4.3–5.0	4.4 \pm 0.3 4.0–4.8	4.5 \pm 0.3 3.7–4.8	4.7 \pm 0.1 4.6–4.8	4.6 \pm 0.1 4.4–4.8
Temperature ($^{\circ}$ C)	12.8 \pm 1.7 10.7–14.5	14.9 \pm 1.6 11.6–17.5	10.8 \pm 1.4 8.5–12.2	13.5 \pm 1.4 10.7–15.1	12.2 \pm 0.6 11.8–12.6	15.6 \pm 2.2 12.1–17.9
EC (μ S cm $^{-1}$)	370 \pm 60 320–460	360 \pm 70 220–470	90 \pm 15 70–115	90 \pm 10 70–115	200 \pm 20 185–215	150 \pm 50 95–270
NO $_3^-$ (μ mol L $^{-1}$)	1040 \pm 300 760–1320	1160 \pm 420 260–1785	30 \pm 50 0–120	20 \pm 40 0–120	510 \pm 20 500–520	260 \pm 270 40–860
NH $_4^+$ (μ mol L $^{-1}$)	0.5 \pm 0.4 0.1–1	0.4 \pm 0.9 0–3.5	3.3 \pm 2.2 1.1–7	5.0 \pm 8.0 0–3–30	0.3 \pm 0.1 0.2–0.3	0.4 \pm 0.5 0–1.5
Fe $^{2+}$ (μ mol L $^{-1}$)	0.8 \pm 0.2 0.7–1.1	0.9 \pm 0.4 0.1–1.9	10.0 \pm 8.2 2.7–25.5	15 \pm 15 0.9–56.6	0.4 \pm 0.2 0.2–0.5	0.7 \pm 0.5 0.2–1.5
O $_2$ (μ mol L $^{-1}$)	250 \pm 90 180–310	220 \pm 70 100–320	20 \pm 20 0–40	20 \pm 30 0–110	170 \pm 0 170–170	100 \pm 80 0–200
CH $_4$ (nmol L $^{-1}$)	30 \pm 3 25–30	50 \pm 25 16–130	480 \pm 630 50–1700	2260 \pm 1900 50–6700	1460 \pm 2010 40–2880	1470 \pm 1500 30–4150
pCO $_2$ (ppmv)	22,050 \pm 2000 19,800–24,270	32,560 \pm 12,000 19,000–60,550	28,100 \pm 11,580 7680–39,000	59,080 \pm 25,060 29,685–116,400	21,530 \pm 5950 17,320–25,740	47,700 \pm 29,590 20,600–103,300
TA (μ mol L $^{-1}$)	85 \pm 2 82–86	92 \pm 30 35–130	95 \pm 40 60–135	65 \pm 30 30–100	83 \pm 2 82–85	60–10 45–75
δ^{13} C-DIC (‰)	–20.7 \pm 1.1 –22 to –19.7	–19.6 \pm 1.3 –21.9 to –17.6	–26.6 \pm 1.3 –27.6 to –24.0	–26.8 \pm 1.0 –28.8 to –25.3	–26.9 \pm 1.4 –27.9 to –25.9	–24.9 \pm 0.7 –25.7 to –23.4
DIC (μ mol L $^{-1}$)	1100 \pm 180 930–1300	1520 \pm 490 820–2590	1500 \pm 550 570–2040	2830 \pm 1080 1650–5370	1160 \pm 315 940–1380	2140 \pm 1200 1020–4480
DOC (μ mol L $^{-1}$)	420 \pm 120 320–590	550 \pm 140 340–880	2230 \pm 1440 575–3670	740 \pm 380 310–1720	310 \pm 50 275–350	420 \pm 100 310–620

Table 4

Values of carbon and ancillary parameters throughout sampling period (Jan. 2014–Jul. 2015) in different types of streams across hydrological seasons. Numbers between brackets are corresponding to the sampling size. For each parameter, the table showed the average \pm standard deviations and the range. We defined four groups that are Cropland_HF/Cropland_BF, Forest_HF/Forest_BF corresponding to streams during high flow (HF) or base flow (BF); in either cropland-affected or forest-dominated land use.

	First-order streams			
	Cropland_HF (22)	Cropland_BF (37)	Forest_HF (23)	Forest_BF (55)
pH	5.9 \pm 0.3 5.4–6.6	6.1 \pm 0.4 5.5–7.0	5.7 \pm 0.6 4.2–6.8	6.1 \pm 0.4 5.0–6.9
Temperature (°C)	10.2 \pm 1.6 6.4–12.1	15.7 \pm 3.9 9.1–25.8	9.0 \pm 1.9 4.8–12	14.6 \pm 3.3 8.1–22.1
EC ($\mu\text{S cm}^{-1}$)	230 \pm 50 145–340	220 \pm 60 75–370	110 \pm 20 80–150	120 \pm 30 70–200
NO ₃ ⁻ ($\mu\text{mol L}^{-1}$)	420 \pm 220 180–950	290 \pm 170 8.5–705	95 \pm 70 0–275	65 \pm 70 0–275
NH ₄ ⁺ ($\mu\text{mol L}^{-1}$)	7.0 \pm 8.4 0.5–38.7	5.5 \pm 6.0 0–25.3	1.7 \pm 1.7 0.3–7.8	1.7 \pm 1.7 0–6.9
Fe ²⁺ ($\mu\text{mol L}^{-1}$)	6.7 \pm 3.8 1.6–15.7	5.4 \pm 4.7 0.1–22	5.7 \pm 3.0 2.6–13.6	8.8 \pm 14.0 0.6–57.1
O ₂ ($\mu\text{mol L}^{-1}$)	290 \pm 50 190–400	290 \pm 40 160–370	300 \pm 40 210–370	270 \pm 60 110–360
CH ₄ (nmol L ⁻¹)	580 \pm 1080 30–4380	390 \pm 880 20–4900	185 \pm 190 40–980	270 \pm 340 20–2370
pCO ₂ (ppmv)	5200 \pm 2370 1040–10,740	4040 \pm 2790 1220–14,080	4200 \pm 2430 1240 \pm 11,690	5200 \pm 5100 1010–27,200
TA ($\mu\text{mol L}^{-1}$)	105 \pm 50 40–300	100 \pm 50 30–255	70 \pm 40 35–195	95 \pm 55 30–280
$\delta^{13}\text{C-DIC}$ (‰)	-20.6 \pm 3.9 -27.6 to -11.3	-16.8 \pm 2.4 -22.3 to -12.4	-22.1 \pm 2.5 -27.6 to -16.8	-18.9 \pm 2.3 -23.1 to -14.0
DIC ($\mu\text{mol L}^{-1}$)	380 \pm 130 1000–650	280 \pm 120 90–600	300 \pm 150 150–750	330 \pm 230 120–1280
DOC ($\mu\text{mol L}^{-1}$)	750 \pm 400 300–2290	520 \pm 230 220–1520	540 \pm 305 260–1725	450 \pm 220 190–1540
TSM (mg L ⁻¹)	9.3 \pm 11.5 0.9–51	3.1 \pm 4.9 0.1–27	2.8 \pm 1.7 0.5–6.6	2.1 \pm 1.7 0.4–8.2
POC (%)	26 \pm 10 15–48	30 \pm 10 16–48	29 \pm 8 20–50	29 \pm 10 12–80
POC ($\mu\text{mol L}^{-1}$)	190 \pm 250 0–1100	65 \pm 100 0.3–540	65 \pm 40 0–170	40 \pm 30 0.5–140

with lower water temperatures while the base flow period was associated with higher water temperatures (Tables 2–4).

3.2. K-means clustering analysis

For both hydrological seasons (i.e., high and base flow), we partitioned each sampling stations (excepting riparian groundwater), into either cropland-affected or forest-dominated waters (Table 1). K-means clustering analysis produced satisfactory results. Logically, groundwater located in cropland was classified as crop water whereas groundwater located in forest was classified as forest water (Table 1). Stream sampling stations having >30% of croplands in their respective catchment were always classified as crop waters (Table 1). Stream sampling stations having <8% of croplands in their respective catchment were always classified as forest waters excepting two times (Table 1). These two stream sampling stations were located a few kilometers downstream from important maize croplands. Specifically, one station was a ditch strongly vegetated during the base flow period that showed signs of N fertilizer uptake from upstream cropland and, therefore, this ditch was logically classified as a crop station during base flow (Table 1). One station was a stream that exhibited a high water flow during the high flow period, which probably increased the upstream cropland influences during this hydrological period and, therefore, this stream was logically classified as a crop station during high flow (Table 1).

Excepting one strictly forested headwater, the other sampled streams were not strictly forested or cropped (Table 1). Consequently,

as explained further, some biogeochemical variability between forest and crop streams was introduced by simple water mixing from two distinct sources: forest groundwater and crop groundwater. We used the term crop stream to indicate a stream classified as a crop-affected one, although such stream was a forest stream affected by cropland rather than a strictly crop stream.

3.3. Land use influence on water composition of shallow groundwater

PCA on the groundwater dataset revealed that groundwater biogeochemical variability was strongly dependent on land use (maize cropland vs. pine forest) and hydrological seasons (base flow vs. high flow) (Fig. 3a, b). The first three PCA dimensions covered 44%, 17.5% and 10.5% of the total variance within the dataset, respectively (Fig. 3a, b).

PCA dimension 1 clearly separated forest groundwater from crop groundwater based on two groups of variables negatively correlated with one another (Fig. 3a). One group of variables was characterized with crop groundwater and was composed of EC, NO₃⁻, $\delta^{13}\text{C-DIC}$, and O₂, whereas the second group of variables was characterized forest groundwater and was composed of DIC, pCO₂, CH₄, Fe²⁺, and NH₄⁺ (Fig. 3a). Indeed, we observed that the yearly average of EC (+270 $\mu\text{S cm}^{-1}$), NO₃⁻ (+1115 $\mu\text{mol L}^{-1}$), $\delta^{13}\text{C-DIC}$ (+6.9‰), and O₂ (+200 $\mu\text{mol L}^{-1}$) were higher in crop groundwater than in forest groundwater and were significantly and positively affected by cropland cover (Table 2; Fig. 4b, c, f, j). Conversely, we observed higher DIC (+1010 $\mu\text{mol L}^{-1}$), pCO₂ (+19,985 ppmv), CH₄ (+1730 $\mu\text{mol L}^{-1}$), Fe²⁺ (+14.1 $\mu\text{mol L}^{-1}$), and NH₄⁺ (+4.1 $\mu\text{mol L}^{-1}$) in forest groundwater than in crop groundwater; these were significantly and positively affected by forest cover (Table 2; Fig. 4d, e, g, h, k). In riparian groundwater, EC, NO₃⁻, $\delta^{13}\text{C-DIC}$, O₂, DIC, pCO₂, and CH₄ exhibited intermediate values between the groundwater of forest and crop sites, whereas Fe²⁺ and NH₄⁺ were low and close to those found in crop groundwater (Table 2; Fig. 4b, c, d, e, f, g, h, j, k).

In crop groundwater, EC, NO₃⁻, $\delta^{13}\text{C-DIC}$, and O₂ were not significantly affected by hydrological seasons (Fig. 3a, S2c, h, j, k, l). However, $\delta^{13}\text{C-DIC}$ (+1.1‰), NO₃⁻ (+120 $\mu\text{mol L}^{-1}$), and DOC (+130 $\mu\text{mol L}^{-1}$) were slightly higher (but not significantly) during base flow compared to high flow (Table 3; Fig. S2c, h, j, k, l). In forest groundwater, pCO₂, DIC, CH₄, and DOC were significantly affected by hydrological seasons (Table 3; Fig. S2g, h, k, l). DOC (+1490 $\mu\text{mol L}^{-1}$) was significantly higher during high flow, whereas pCO₂ (+30,980 ppmv), DIC (+1330 $\mu\text{mol L}^{-1}$) and CH₄ (+1780 nmol L⁻¹) were significantly higher during base flow (Table 3; Fig. S2 and S4g, h, k, l). In crop and riparian groundwater, we also observed higher pCO₂ and DIC values during base flow, but with lower intensities than in forest groundwater (Table 3; Fig. S2h, k).

3.4. Land use influence on water composition of first-order streams

Fig. 3c–d present PCA based on first-order streams data set. The first three PCA dimensions covered 28.6%, 18.5% and 13.8% of the total variance within the dataset, respectively (Fig. 3c, d).

Interestingly, the PCA based on the first-order streams dataset did not clearly separate crop streams from forest streams as it did for groundwater dataset (Fig. 3a–d). This implied lower spatial variability in streams in relation to land use in than in groundwater (Tables 2–4; Fig. 4). Nevertheless, a land use gradient was observed on PCA dimension 2 (Fig. 3c, d). PCA dimension 2 was best defined by a group of variables composed of EC, CH₄, NO₃⁻, NH₄⁺, DOC, TSM, and POC, which collectively characterized crop streams (Fig. 3c, d). On a yearly average basis, significantly higher EC (+105 $\mu\text{S cm}^{-1}$), CH₄ (+220 $\mu\text{mol L}^{-1}$), NO₃⁻ (+265 $\mu\text{mol L}^{-1}$), NH₄⁺ (+4.3 $\mu\text{mol L}^{-1}$), DOC (+135 $\mu\text{mol L}^{-1}$), TSM (+3.3 mg L⁻¹), and POC (+70 $\mu\text{mol L}^{-1}$) were observed in crop streams compared to forest streams (Table 2; Fig. 4b, c, d, g, l, m, o). High CH₄, NH₄⁺, and DOC

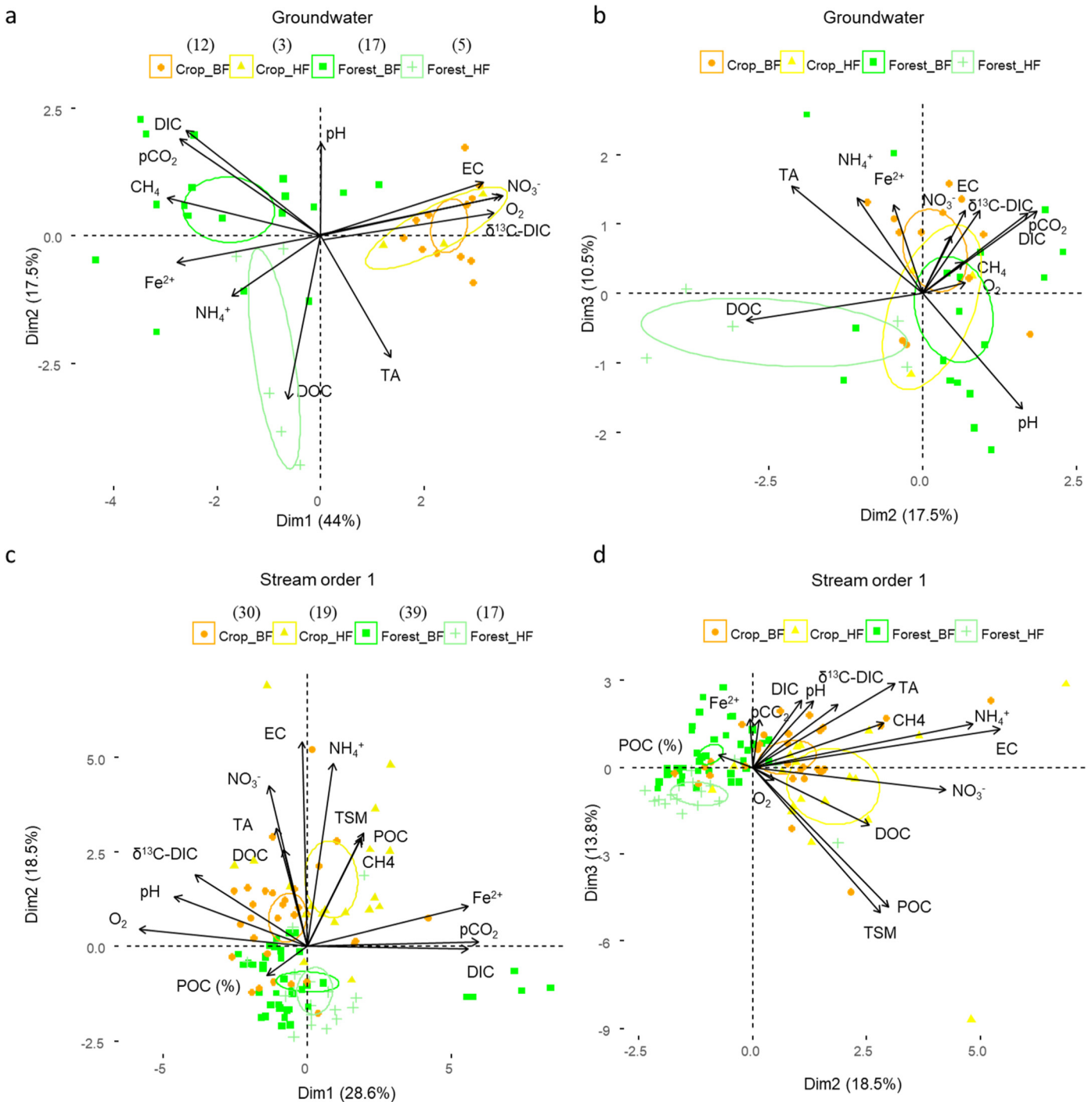


Fig. 3. Principal component analysis (PCA) of shallow groundwater dataset (a–b) and first-order streams dataset (c–d). We represented only the first three dimensions. Numbers between brackets are corresponding to the sampling size. The sampling size in the PCAs did not correspond exactly to the sampling size in Tables 3 and 4 because R software deletes stations from the analysis with a missing value for one parameter. In these PCAs, we used all the quantitative variables measured in this study. In each PCA, we plotted as well the individuals separated in four groups. The first group corresponds to cropland-affected samples during high flow (Crop_HF), the second group corresponds to cropland-affected samples during base flow (Crop_BF), the third group corresponds to forest-dominated samples during high flow (Forest_HF) and the fourth group corresponds to forest-dominated samples during base flow (Forest_BF). The mean value of each qualitative group has 95% chance to be within the corresponding confidence ellipse.

concentrations were characteristics of forest groundwater, but in streams, these parameters were characteristic of crop streams (Fig. 3a–d). In addition, $p\text{CO}_2$, DIC, $\delta^{13}\text{C-DIC}$ and O_2 were not able to separate crop streams from forest streams as they did for groundwaters (Fig. 3a–d). On a yearly average basis, no significant differences were observed between crop and forest streams for these four parameters (Fig. 3f, h, j, k).

The relatively low temporal variability between high and base flow periods observed in both crop and forest streams for the studied parameters did not allow the PCA based on stream data set to clearly separate base flow samples from high flow samples (Table 4; Figs. 3c–d, S3, S4). Nevertheless, in crop streams, pH (+0.2) and $\delta^{13}\text{C-DIC}$ (+3.8‰) were significantly higher during base flow while $p\text{CO}_2$ (−1160 ppmv), NO_3^- (−130 $\mu\text{mol L}^{-1}$) and DOC (−230 $\mu\text{mol L}^{-1}$) were significantly lower

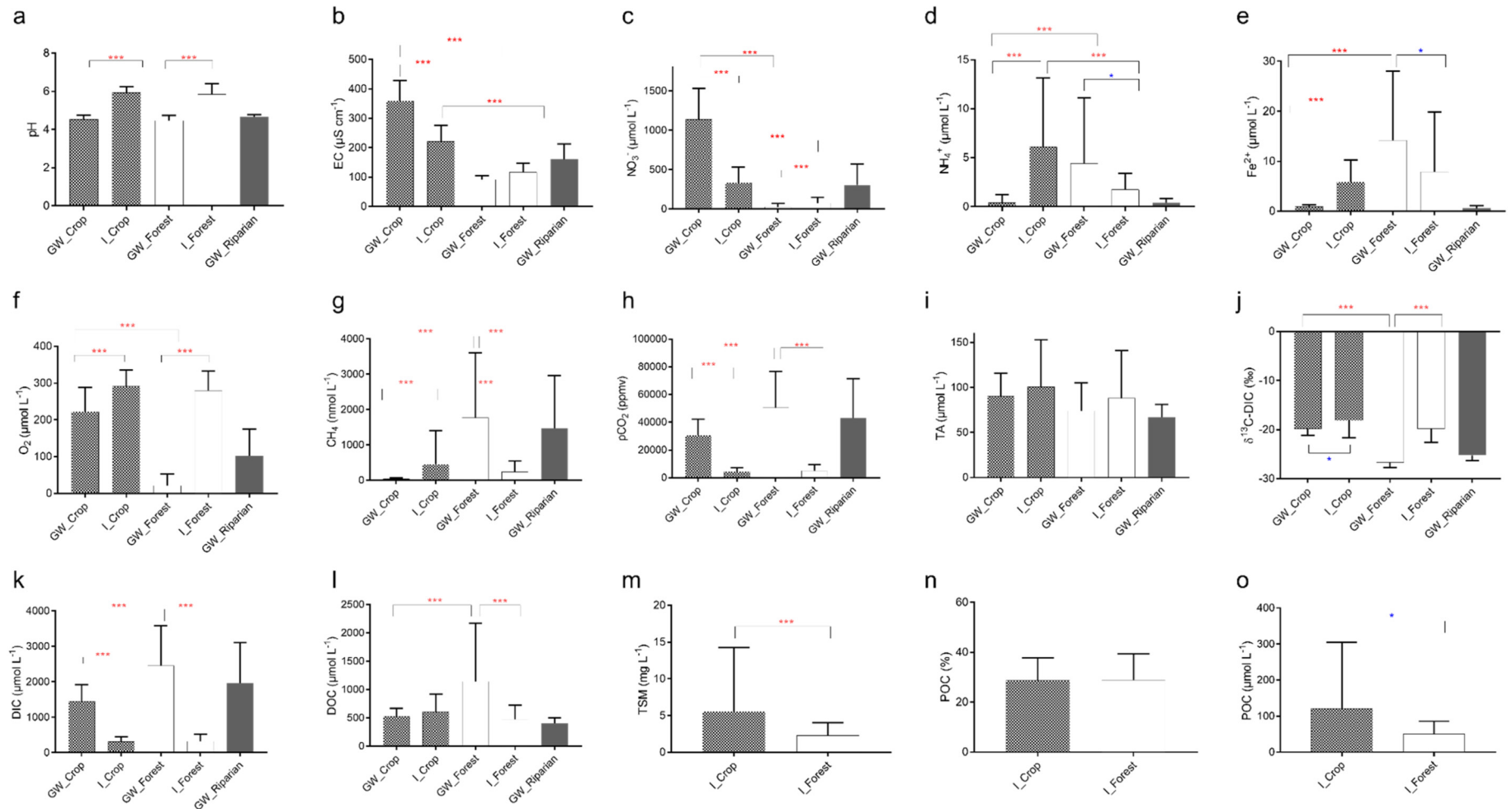


Fig. 4. Values of carbon and ancillary parameters throughout the sampling period (Jan. 2014–Jul. 2015) in groundwater and streams across land use. Histograms represent the mean with standard deviations of a given parameter. We defined four groups that are GW_Forest/GW_Crop and L_Forest/L_Crop corresponding to groundwaters and streams order 1 either dominated by forests or croplands. A fifth group is GW_Riparian and corresponding to riparian groundwater. Then, based on Mann-Whitney statistical analysis, we compared GW_Crop VS L_Crop, GW_Forest VS L_Forest, GW_Crop VS GW_Forest, L_Crop VS L_Forest. Three red stars (***) indicate that data were significantly different with $p < 0.001$. One blue star (*) indicates that data were significantly different with $p < 0.05$. No stars indicate that data were not significantly different ($p > 0.05$).

during the same period (Table 4; Fig. S3a, j, c, h, l, m, o). In streams, TSM and POC were significantly higher during high flow but with a higher intensity in crop streams than in forest streams (Table 4; Fig. S3m, o). Interestingly, in both forest and crop streams, POC% was not significantly affected by hydrological regime (Table 4; Fig. S3n).

3.5. Upstream-downstream distribution of biogeochemical parameters

To explore the influence of land use on water composition at the groundwater-stream continuum, we observed the upstream-downstream (groundwater-stream) distribution of biogeochemical parameters along forest and crop continuums (Table 2; Fig. 4). Along both types of continuum, some parameters (i.e., pCO_2 , TA, DIC, $\delta^{13}C$ -DIC, pH, O_2) exhibited the same upstream-downstream distribution, whereas other parameters (i.e., EC, NO_3^- , NH_4^+ , Fe^{2+} , CH_4 , DOC) exhibited a different upstream-downstream distribution (Table 2; Fig. 4).

In crop and forest continuums, we observed strong spatial patterns for pCO_2 , TA, DIC, $\delta^{13}C$ -DIC, and pH: pCO_2 and DIC decreased while TA remained more or less constant, and $\delta^{13}C$ -DIC and pH increased (Table 2; Fig. 4a, h, i, j, k). However, a larger decrease in pCO_2 levels in the forest continuum suggested a more intense degassing in forest streams (Table 2; Fig. 4h). We also observed an increase in O_2 in both types of continuum, which could result from stream ventilation, although with a higher intensity in forest continuum (Table 2; Fig. 4f, h).

EC decreased downstream in the crop continuum, but did not in the forest continuum where EC remained very stable and much lower than in the crop continuum (Table 2; Fig. 4b). NO_3^- decreased downstream between groundwater and streams in croplands, and in contrast, in forests NO_3^- increased downstream between groundwaters and streams (Table 2; Fig. 4c). NH_4^+ , Fe^{2+} , and CH_4 decreased in the forest continuum

but they increased in the crop continuum (Table 2; Fig. 4d, e, g). DOC significantly decreased in the forest continuum but remained stable in the crop continuum (Table 2; Fig. 4l). TSM and POC were significantly higher in crop relative to forest streams; however, similarly high POC% (28%) was observed in both types of streams (Table 2; Fig. 4m, n, o).

3.6. Biogeochemistry dynamics in the groundwater-stream continuum

PCA with groundwater and streams datasets indicated mathematically that streams were fed with two distinct sources: forest groundwater mostly characterized by high pCO_2 , DIC, and CH_4 concentrations and crop groundwater mostly characterized by high NO_3^- concentrations (Fig. 5). Forest and crop streams were characterized by higher O_2 , $\delta^{13}C$ -DIC and pH values than in groundwater (Fig. 5). In this PCA, the distinction between forest and crop streams was primarily a function of NO_3^- , crop streams points were moved upward along dimension 2 (Fig. 5). Throughout the sampling period, we observed a negative linear relationship ($R^2 = 0.6$, $p < 0.001$, $n = 192$) between CO_2 and O_2 for all sampled groundwater and streams (Fig. 6a). On the one side, stream samples were mostly characterized by high O_2 (mean was $290 \mu mol L^{-1}$) and low CO_2 (mean was 4480 ppmv), excepting some forest streams during summer that were characterized by low O_2 (down to $110 \mu mol L^{-1}$) and high CO_2 (up to 27,200 ppmv) (Table 2; Fig. 6a, S4f, h). On the other side, anoxic conditions associated with high CO_2 (mean was 50,630 ppmv) were characteristic of forest groundwater, whereas crop groundwater exhibited O_2 (mean was $220 \mu mol L^{-1}$) and CO_2 (mean was 30,650 ppmv) intermediate between streams and forest groundwater (Table 2; Fig. 6a). In forest groundwater, DOC was negatively and linearly correlated with CO_2 ($R^2 = 0.4$, $p < 0.001$, $n = 22$) suggesting that part of groundwater CO_2 came from degradation

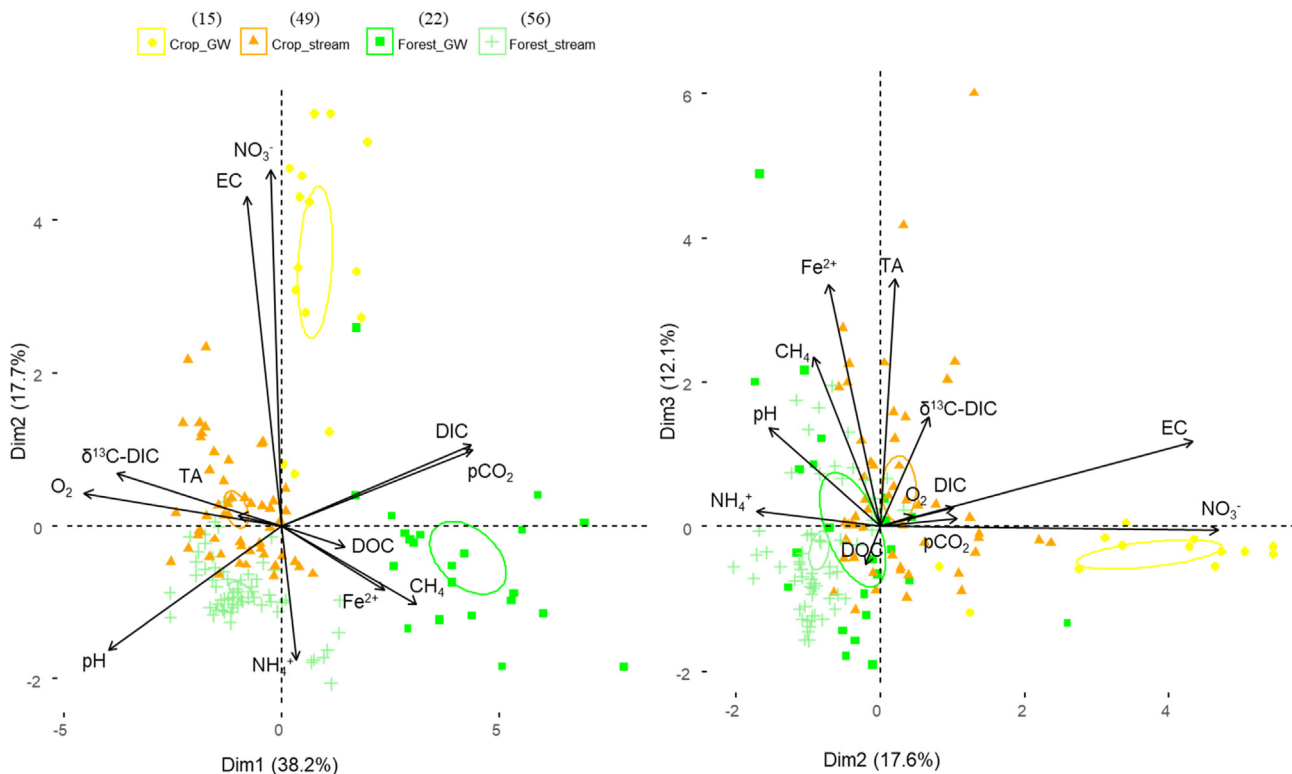


Fig. 5. Principal component analysis (PCA) of shallow groundwater and stream datasets. We represented only the first three dimensions. Numbers between brackets are corresponding to the sampling size. The sampling size in the PCA did not correspond exactly to the sampling size in Table 2 because R software deletes stations from the analysis with a missing value for one parameter. In these multivariate statistical analyses, we used all the quantitative variables measured in this study. We defined four groups that are Crop_GW/Forest_GW and Crop_stream/Forest_stream, which are corresponding to groundwater and streams order 1, either dominated by forests or croplands. The mean value of each qualitative group has 95% chance to be within the corresponding confidence ellipse.

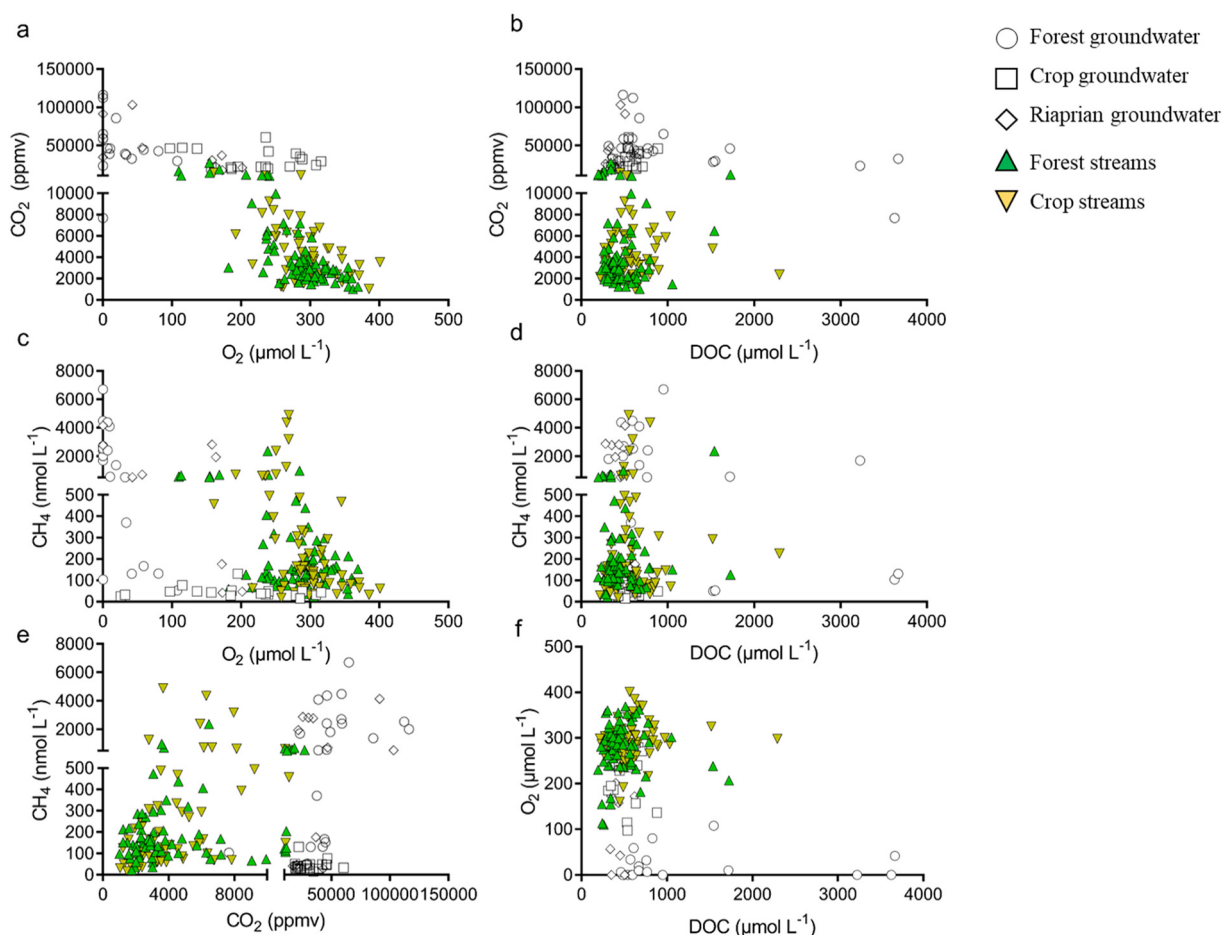


Fig. 6. Scatter plots of (a) CO_2 (ppmv) vs. O_2 ($\mu\text{mol L}^{-1}$), (b) CO_2 (ppmv) vs. DOC ($\mu\text{mol L}^{-1}$), (c) CH_4 (nmol L^{-1}) vs. O_2 ($\mu\text{mol L}^{-1}$), (d) CH_4 vs. DOC ($\mu\text{mol L}^{-1}$), (e) CH_4 (nmol L^{-1}) vs. CO_2 (ppmv), and (f) O_2 ($\mu\text{mol L}^{-1}$) vs. DOC ($\mu\text{mol L}^{-1}$), in all sampled groundwater and streams.

of groundwater DOC (Fig. 6b). A comparison of CO_2 and CH_4 for all sampled groundwaters and streams showed that a large portion of the CO_2 and CH_4 in forest streams could come from forest groundwater discharge (Table 2; Fig. 6e). In crop streams, CH_4 , NH_4^+ , and Fe^{2+} could not originate from crop groundwater discharge since they had much lower CH_4 , NH_4^+ , and Fe^{2+} concentrations than crop streams (Table 2; Fig. 6c, 7d, f). We observed a positive linear relationship between CH_4 and NH_4^+ ($R^2 = 0.4$, $p < 0.001$, $n = 53$) in crop streams, demonstrating that these two compounds may come from the same source (Fig. 7d). Conversely, a comparison of O_2 and NH_4^+ or Fe^{2+} in forest streams indicated that NH_4^+ and Fe^{2+} were mostly discharged through forest groundwater (Fig. 7b, f). In forest streams, the negative linear relationship between O_2 and NH_4^+ ($R^2 = 0.1$, $p\text{-value} < 0.05$, $n = 70$), Fe^{2+} ($R^2 = 0.5$, $p\text{-value} < 0.001$, $n = 77$), or CH_4 ($R^2 = 0.1$, $p\text{-value} < 0.001$, $n = 77$) suggested oxidation of these reduced compounds in the stream water column (Fig. 6c, 7b, f). We observed a gradient of NO_3^- concentration, from high values to low values, between crop groundwater (mean was $1140 \mu\text{mol L}^{-1}$), to riparian groundwater and crop streams (310 and $340 \mu\text{mol L}^{-1}$, respectively), to forest streams ($75 \mu\text{mol L}^{-1}$) and to forest groundwater ($25 \mu\text{mol L}^{-1}$) (Table 2; Fig. 7a, c, e). In crop streams, a large share of riverine NO_3^- could be discharged through crop groundwater. Conversely, NO_3^- concentration in forest streams could not be explained by NO_3^- concentration in forest groundwater (Table 2; Fig. 7a, c, e). In crop groundwater, high NO_3^- concentrations were associated with low CH_4 concentrations. In crop streams, high NO_3^- concentrations could be related to high CH_4 concentrations (Fig. 7c).

4. Discussion

4.1. Water table depth in relation to land use

At the studied catchment scale, lithology, topography, soils, and precipitation are more or less uniform (Augusto et al., 2010; Jolivet et al., 2003). At the plot scale, spatial variability of water table depth in relation to land use was thus necessarily dependent on how water outputs (drainage, evapotranspiration or groundwater storage) of the water mass balance were human-affected (Govind et al., 2012; Stella et al., 2009). Local forests are never irrigated, conversely, irrigation with extraction of groundwater (that decreases groundwater storage) in local croplands could strongly bias the water mass balance at the plot scale since about half of the water diverted for irrigation is rapidly consumed through evapotranspiration (e.g., Jackson et al., 2001). Additionally, evapotranspiration in maize croplands is typically higher than in forests owing to the larger stomatal conductance that makes the exchange of C and water between the biosphere and the atmosphere much easier (Govind et al., 2012; Stella et al., 2009). Other studies have shown that the combination of subsoiling practices (increasing soil permeability) with deep agricultural ditches in croplands also affected water mass balance at the plot scale by enhancing lateral drainage of groundwater (Evans et al., 1996; Robinson et al., 1985). From an 8 year survey of local cropland, Juste et al. (1982) showed that lateral drainage strongly affected the water mass balance at the plot scale as it represented an annual mean of 637 mm (70% of the amount of precipitation), whereas precipitation was estimated at 922 mm . At the forest plot scale, lateral

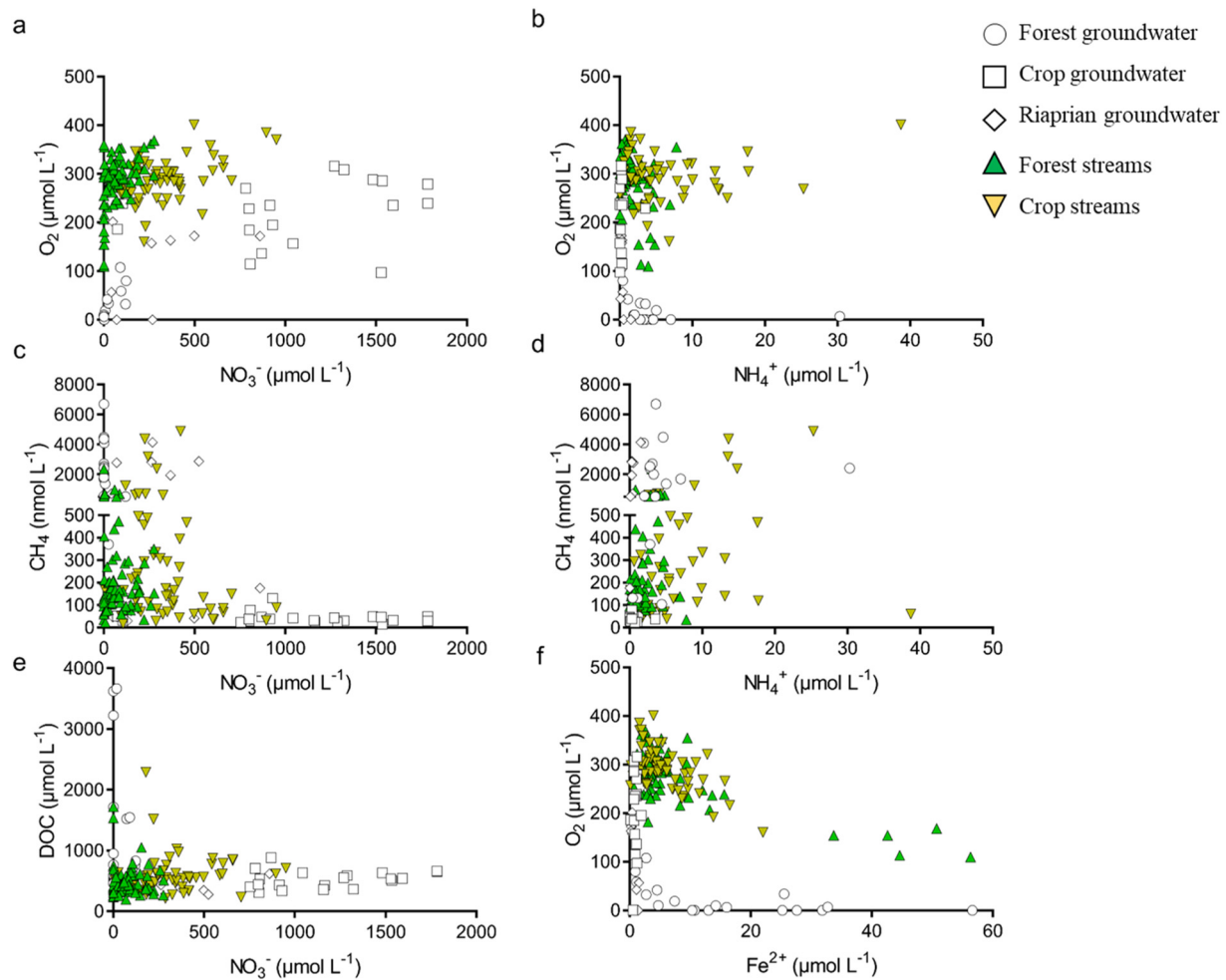


Fig. 7. Scatter plots of (a) O₂ (μmol L⁻¹) vs. NO₃⁻ (μmol L⁻¹), (b) O₂ (μmol L⁻¹) vs. NH₄⁺ (μmol L⁻¹), (c) CH₄ (μmol L⁻¹) vs. NO₃⁻ (μmol L⁻¹), (d) CH₄ (μmol L⁻¹) vs. NH₄⁺ (μmol L⁻¹), (e) DOC (μmol L⁻¹) vs. NO₃⁻ (μmol L⁻¹), and (f) O₂ (μmol L⁻¹) vs. Fe²⁺ (μmol L⁻¹), in all sampled groundwater and streams.

drainage represented an annual mean of 182 mm (20% of the amount of precipitation), whereas precipitation was estimated at 895 mm (Deirmendjian et al., 2018). At the study site, deeper water table in croplands was thus a consequence of a higher evapotranspiration and more lateral drainage than in forest. As explained further, water table depth is an important determinant for understanding the biogeochemical variability in groundwater in relation to land use.

4.2. Dynamic of O₂, DOC, DIC and δ¹³C-DIC in groundwater: A combination of hydrological, physical and metabolic processes

In other aquifer systems worldwide, several studies have observed a significant positive correlation between groundwater O₂ concentration and depth to water (Datry et al., 2004; Foulquier et al., 2010; Goldscheider et al., 2006; McMahon and Chapelle, 2008; Pabich et al., 2001). Where the water table is close to the soil surface, groundwater O₂ consumption is likely rapid because of incomplete degradation of soil-generated labile DOC in the unsaturated zone. On the contrary, where the water table is far from the soil surface, strong oxygen depletion in the vicinity of the water table does not occur since the higher residence time of infiltrating water results in almost complete degradation of soil-generated DOC in the unsaturated zone (Malard and Hervant, 1999; Starr and Gillham, 1993). A regional study in forest soils of Switzerland (Hagerdon et al., 2000) and a study compiling a global database of soil carbon (Camino-Serrano et al., 2014) both found that soil-generated DOC was preferentially mobilized under reducing conditions

in soils because of dissolution of Fe oxides. Deeper water tables in croplands do not reach topsoil that exhibits high labile organic C content. Thus, reducing conditions in topsoil and the leaching of soil-generated DOC are prevented as is the consumption of the groundwater O₂ stock, as occurs in forests during high flow stages (Table 3; Fig. S2l; Deirmendjian et al., 2018). Therefore, groundwater pCO₂ was higher in the forest during high flow than it was in cropland and riparian sites (Table 3; Fig. 4h, S2l, h). This also explains the negative correlation between DOC and CO₂ observed only in forest groundwater (Fig. 6b). During base flow, we observed a clear land use spatial pattern among cropland, riparian forest, and forest sites (Table 3; Fig. S2h). We hypothesize that this difference was a consequence of a less intense soil respiration in croplands during summer. From simultaneous eddy covariance measurements over pine forests and maize croplands of the study area, Stella et al. (2009) confirmed that ecosystem respiration was lower in croplands than in forests over the whole year. However, Stella et al. (2009) also showed that ecosystem respiration was larger during the growing season of the maize, because of increased soil respiration in response to the higher soil water content caused by irrigation. In forest sites, groundwater pCO₂ increases during the summer because soil CO₂ diffuses downward and then is dissolved into the water table (Deirmendjian et al., 2018; Tsy-pin and Macpherson, 2012). A deeper water table in cropland suggests a less efficient CO₂ transfer from soil air to water table. Higher soil moisture in croplands due to irrigation probably delays soil CO₂ diffusion to groundwater.

The $\delta^{13}\text{C}$ -DIC signature of forest groundwater was typical of a signature that originated from respiration of soil organic matter derived from C_3 plants (O'Leary, 1988; Vogel et al., 1993). The studied forest soils have no natural carbonate minerals (Augusto et al., 2010) and DIC originating from silicate weathering has the same isotopic signature as DIC originating from soil respiration (Das et al., 2005; Polsemaere and Abril, 2012; Wachniew, 2006). Crop groundwater had a heavier $\delta^{13}\text{C}$ -DIC signature than forest groundwater and this discrepancy resulted from distinct processes. Liming in cropland brings artificial carbonates into crop soil and DIC originating from carbonate weathering produced DIC with a $\delta^{13}\text{C}$ value of approximately half of that of soil CO_2 as carbonate rocks have a $\delta^{13}\text{C}$ of approximately 0‰, making $\delta^{13}\text{C}$ -DIC less negative (Clark and Fritz, 1997; Salomons and Mook, 1986). Irrigation with extraction of groundwater could also increase the $\delta^{13}\text{C}$ -DIC signature by enhancing the degassing rate of $^{12}\text{CO}_2$ relative to $^{13}\text{CO}_2$ (Deirmendjian and Abril, 2018; Polsemaere and Abril, 2012). Changes in the $\delta^{13}\text{C}$ -DIC signature could also originate from respiration of soil organic matter derived from maize, a C_4 plant with a heavier $\delta^{13}\text{C}$ signature than C_3 forest plants (O'Leary, 1988; Vogel et al., 1993), as observed in the study region (Quénéa et al., 2006). Indeed, after three decades of cultivation, the remaining carbon from the forest pool was mostly recalcitrant and its degradation probably did not affect the $\delta^{13}\text{C}$ -DIC pool (Jolivet et al., 1997).

4.3. Dynamics of IN and CH_4 in groundwater: The influence of groundwater O_2

Subsurface and groundwater redox zonation is driven by the spatial and temporal distribution of O_2 that serves as the primary terminal electron acceptor during the degradation of organic C. In crop groundwater, high O_2 concentrations inhibited methanogenesis, as this process is strictly anaerobic and thus resulted in very low CH_4 concentrations (Table 2; Fig. 4f, g; Borges et al., 2018; Ciais et al., 2010; Jurado et al., 2017; Klüber and Conrad, 1998). Conversely, forest and riparian groundwater exhibited anoxic conditions that allowed methanogenesis to occur and created higher CH_4 concentration in forest sites compared to cropland sites (Table 2; Fig. 4f, g). High water table stages in forested areas cause anoxia in soils, forcing plants and microorganisms to switch to anaerobic metabolism (Naumburg et al., 2005; Bakker et al., 2006, 2009). Thus, in riparian and forest areas, we expected a positive relationship between water table and groundwater CH_4 but, to the contrary, we observed a negative relationship between these two parameters ($R^2 = 0.25$, $p < 0.05$; data not shown). This implies that methanogenesis primarily occurs in deeper layers of forest soils, especially in summer. Fe^{2+} and NH_4^+ accumulates in forest groundwater because anoxic conditions inhibit nitrification and iron oxidation (Table 2; Fig. 4d, e; Jambert et al., 1994; Widdel et al., 1993).

In groundwater, anoxic conditions enable heterotrophic denitrification, whereas an O_2 threshold of 30–60 $\mu\text{mol L}^{-1}$ completely inhibits heterotrophic denitrification (Balestrini et al., 2016; Cey et al., 1999; Christensen et al., 2013; Jambert et al., 1994; Kolbjørn Jensen et al., 2017; Korom, 1992). In strictly forest sites, denitrification in groundwater is usually limited by the scarcity of NO_3^- , whereas in strictly crop sites denitrification is often limited by organic C availability (Table 2; Jambert et al., 1994; Starr and Gillham, 1993). Thus, N fertilizer application associated with different groundwater denitrification rates in the different plots creates the observed spatial pattern of groundwater NO_3^- concentration in crop, riparian and forest sites (Table 2; Fig. 4c). In local maize croplands, Jambert et al. (1997) found that 13% of the N fertilizers inputs were converted to N_2 gas, demonstrating that denitrification could occur in these oxic crop soils and groundwater. Although oxic conditions are not favorable for groundwater denitrification, some studies in agricultural catchments do describe this process at relatively high O_2 (150 $\mu\text{mol L}^{-1}$) levels (McAleer et al., 2017; Otero et al., 2009). In crop soils, Rubol et al. (2016) investigated the spatio-temporal dynamics in oxidative microbial activity and the development

of anoxic micro zones (i.e., anoxic hot-spots) at the microscopic level (μm to cm). They found that labile C addition resulted in maximum rates of local metabolic activity within a few minutes and led to the subsequent formation of anoxic hotspots and thus, both oxic and anoxic conditions coexisted closely within a small volume of crop soils. Consequently, denitrification probably occurs in anoxic microsites in water-logged soil during irrigation as higher soil moisture results in lower soil oxygen concentration, lower redox potential and higher leaching of soil DOC (Hagedorn et al., 2000; Jambert et al., 1997; Rubol et al., 2012; Silver et al., 1999).

N fertilizer load in local croplands is 25 $\text{g N m}^{-2} \text{yr}^{-1}$ (Jambert et al., 1997), whereas export (using drainage of 637 mm yr^{-1} and the average NO_3^- concentration in crop groundwater) of NO_3^- through crop groundwater was estimated at 10 $\text{g N m}^{-2} \text{yr}^{-1}$ (40% of the annual N fertilizer load), and export (using same drainage and the average NO_3^- concentration in riparian groundwater) of NO_3^- through riparian groundwater was estimated at 2.8 $\text{g N m}^{-2} \text{yr}^{-1}$ (8% of the annual N fertilizer load). This shows the importance of riparian groundwater to attenuate N inputs from adjacent croplands to streams, otherwise a large portion of the annual N fertilizer load would have been leached into adjacent streams rather than being denitrified or used by plants. In riparian groundwater adjacent to a farm in the New York state (USA), Anderson et al. (2014) found that total groundwater denitrification was equivalent to 32% of manure N spread on the adjacent upland field. Mekala et al. (2017) simulated the transport and dynamics of N in an agricultural soil under flooded conditions and concluded that relatively shallow aquifers with sandy soil are vulnerable to NO_3^- contamination at around 10 days if continuous irrigation is practiced. They also stated that NO_3^- had higher leaching potential than NH_4^+ or DOC. At our study site, irrigation and associated desorption of DOC and NO_3^- could explain their slight increase in crop groundwater during base flow (Table 3, Fig. 1, S2c). In a storm infiltration basin in Florida (USA), O'Reilly et al. (2012) found that concomitant peaks in groundwater O_2 and NO_3^- concentrations after storm rainfall were a consequence of organic N leaching, indicating that there were short periods of ammonification and nitrification. In crop groundwater of Wallonia (Belgium), when groundwater O_2 levels are higher than 125 $\mu\text{mol L}^{-1}$ (as at the study site), nitrification rather than denitrification promotes the accumulation of N_2O in groundwater (Jurado et al., 2017).

4.4. Stream biogeochemical functioning: Mostly a function of groundwater composition

NO_3^- inputs to streams cause stream eutrophication (Carpenter et al., 1998; Jordan and Weller, 1996; Smith, 2003; Zhou et al., 2017). This is consistent with our field observations where we observed that crop streams were highly vegetated with macrophytes during base flow stages. Compared to high flow conditions, crop stream eutrophication was accompanied by higher pH and $\delta^{13}\text{C}$ -DIC, and lower pCO_2 caused by preferential $^{12}\text{CO}_2$ uptake during the macrophyte plant photosynthesis (Table 4; Fig. S3a, h, j; De Carvalho et al., 2009; Raven et al., 2002). The development of macrophytes in crop streams modifies flow and can cause a significant drop in water velocity, which in turn, gives rise to extensive deposition and retention of sediment beneath the macrophytes (Cotton et al., 2006; Sand-Jensen and Pedersen, 1999). This leads to seasonal accumulation of organic matter, a predominance of anoxic conditions in stream sediments, and thus the occurrence of methanogenesis as evidenced by peaks in dissolved CH_4 during base flow (Table 4; Fig. S3g; Borges et al., 2018; Crawford et al., 2016; Sanders et al., 2007). Crop stream CH_4 concentration was 390 nmol L^{-1} during base flow (Table 2), a concentration significantly lower (1430 nmol L^{-1}) than chalk streams impacted by macrophyte vegetation in England (Sanders et al., 2007). This discrepancy probably resulted from the increased in silt and clay fraction during summer of the underlying sediment in chalk streams (Sanders et al., 2007). This would suggest that the permeability of chalk stream sediment became

lower than that of sandy stream sediment and created stronger reducing conditions in chalk stream sediments, which likely increased the potential for methanogenesis (Baker et al., 1999; Findlay, 1995; Kankaala et al., 2005; Morrice et al., 1997). Sanders et al. (2007) also showed that the chalk streams' emissions of CH₄ to the atmosphere were approximately 50 times lower than the CH₄ production in stream sediments, illustrating the high potential for CH₄ oxidation in the water column of crop stream. During base flow, a second explanation for higher CH₄ (and NH₄⁺) concentrations in crop streams relative to forest streams could be differential hydrology. Drainage plot is a function of the water table height (hydraulic gradient, Darcy's law). During base flow, the water table in cropland was deeper than in forest (e.g., 4 m deeper in Sep. 2014; Fig. 2), and so during this period, potentially more forest groundwater was drained into crop streams. However, in forest streams we usually did not observe CH₄ (or NH₄⁺) concentrations as high as in crop streams (Table 2; Fig. 7d) indicating that CH₄ (or NH₄⁺) in crop streams primarily originated from crop stream sediments rather than from higher discharge of forest groundwater. In crop streams, CH₄ was correlated with NH₄⁺ but not correlated with NO₃⁻ or DOC (Figs. 6d, 7c, d). Such relationships were also observed in the Meuse river basin (Belgium) (Borges et al., 2018) and in a global meta-analysis of riverine CH₄ (Stanley et al., 2016). In contrast, this does not fit the conceptual model of Schade et al. (2016) developed from data in New Hampshire streams, whereby the CH₄ was positively correlated with DOC, while negatively related to NO₃⁻.

Sandy sediments of low order stream beds impacted by eutrophication are significant areas of NO₃⁻ reduction over the spring and summer, lowering DOC and NO₃⁻ concentrations in stream water (Table 4; Fig. S3c, l; Böhlke et al., 2009; Mulholland et al., 2008; Sanders et al., 2007). Additionally, the decreased of stream velocity during base flow increased residence times of NO₃⁻ in the hyporheic zone and the time for denitrification (Bardini et al., 2012). In a small stream dominated by maize cropland in the USA, Böhlke et al. (2009) demonstrated that denitrification mainly occurred in sediments and not in the water column since integrated rates of pore-water denitrification derived from ¹⁵N tracer profiles within the hyporheic zone were similar to the reach-scale rates derived from measurements in the stream. In crop streams, a portion of the NO₃⁻ variability between the two hydrological periods could also result from higher drainage of forest groundwater during base flow, which would dilute the NO₃⁻ signal from crop groundwater.

Considering the flat catchment topography, a minor portion of TSM and POC in streams originates from soil erosion and surface runoff. The most frequent effects of dredging on aquatic ecosystems are changes in the concentration of suspended solids, turbidity and light penetration (Lewis et al., 2001; Newell et al., 1998). Higher concentrations of POC (and TSM) observed in crop streams were also caused by macrophyte biomass developed in summer became a sediment trap. When stream discharge was sufficiently energetic, it re-suspended all the accumulated sediment and removed this litter. Moreover, we observed peaks of CH₄ and NH₄⁺ in crop streams during high flow (Table 4; Fig. S3d, g), suggesting that dredging or streambed erosion of crop streams also release CH₄ and NH₄⁺ from the sediment.

In forest streams, we observed significantly lower concentrations of Fe²⁺, NH₄⁺, and CH₄ than in forest groundwater and significant negative linear relationships between O₂ on the one side and Fe²⁺, NH₄⁺, or CH₄ (Table 2; Figs. 4d, e, g, 7d, f). This suggests there were low O₂ concentration groundwater inputs with high concentrations of reduced compounds and that the stream water was gradually oxygenated, which induced Fe²⁺ and CH₄ oxidations and nitrification. Mulholland et al. (2000) studied N cycling by adding ¹⁵N-labeled NH₄⁺ into a forest stream in eastern Tennessee (USA). They concluded that the residence time of NH₄⁺ in the water column was low (5 min) and that nitrification was an important sink for NH₄⁺, accounting for 19% of total ammonium uptake. In forest streams, the NH₄⁺ concentration was approximately 3 μmol L⁻¹ lower than in forest groundwater and thus did not explained

the NO₃⁻ increase of 50 μmol L⁻¹ (Table 2; Fig. 3c, d). Up to 76% of N exports from local forest are in organic forms but these N exports are very low (<0.2 g N m⁻² yr⁻¹; De Wit et al., 2005; Rimmelin, 1998; Vernier et al., 2003), so in-stream mineralization of organic N coupled to nitrification could not explain NO₃⁻ concentrations in forest streams. Since the sampled forest streams are not strictly forested, NO₃⁻ concentration are explained by simple hydrological mixing between crop and forest groundwater (Table 2).

In streams, pCO₂ was lower and O₂ was higher than in groundwater (Table 2; Figs. 3f, h, 6a). This shows that gas exchange between stream water and the atmosphere occurs quickly, favored by low stream depth and strong concentration gradients between the two compartments. Some authors (e.g., Bodmer et al., 2016; Borges et al., 2018) found elevated pCO₂ in crop streams rather than in forest streams, due to higher levels of dissolved and particulate organic matter in crop dominated systems compared to the forested ones that facilitated the in-stream degradation of organic matter. Moreover, land uses are expected to change the composition of terrestrial soil organic matter leached to streams, shifting from vegetation- to microbe-derived organic matter with greater agricultural land use and potentially higher emissions in crop streams (Fuss et al., 2017; Graeber et al., 2015; Wilson and Xenopoulos, 2009). Those results contrasted with ours because we found no difference in pCO₂ between crop and forest streams. Forest groundwater did have higher pCO₂ than crop groundwater, indicating a more intense degassing in forest streams. The similar δ¹³C-DIC signatures in forest and crop streams despite the strong difference between crop and forest groundwater suggests faster isotopic equilibration of DIC resulting from degassing. The greater gas transfer velocity in forest streams is a consequence of the abundance of coarse woody debris which generates higher levels of water turbulence (e.g., Bodmer et al., 2016), and is consistent with our field observations. A lower gas transfer velocity lower in crop streams results from stream calibration reducing turbulent flow, and macrophyte vegetation that protects the water surface from wind shear.

5. Conclusion

The present study demonstrates that C and IN concentrations in shallow groundwater and in first-order streams are strongly sensitive to land use. In sandy lowland catchments, simultaneous measurements of biogeochemical parameters in groundwater and streams are crucial for identifying and quantifying biogeochemical processes involved at the groundwater-stream interface. We also show that a statistical clustering analysis based on NO₃⁻ dataset enables partitioning of groundwater and streams into crop-affected or forest-dominated waters. Such a classification could be useful to river managers and policy makers. The water table had greater depth in croplands and was a crucial parameter necessary for understanding groundwater biogeochemical variability in relation to land use. Higher water table stages in forests created anoxic conditions and increased soil leaching. Conversely, in croplands, the deeper water table prevented anoxic conditions, creating different groundwater compositions from forest groundwater and inhibiting the denitrification of the N fertilizers, which led to groundwater NO₃⁻ accumulation. Despite the occurrence of groundwater denitrification in riparian and forest sites, N fertilizers inputs in crop streams were still high enough to generate eutrophic conditions in these streams. Eutrophication resulted in a biogeochemical cascading effect, which sustained high CH₄ concentration and lowered NO₃⁻. High CO₂ and CH₄ production occurs in forest soils and groundwater, but these two gases exhibit lower concentrations in forest streams, indicating intense degassing or oxidation.

The groundwater-stream interface is a biogeochemical hotspot and hot moment for C emissions and N removal processes (McClain et al., 2003). Future studies focusing on the groundwater-stream interface in relation to land use are needed to better understand C and N dynamics

in aquatic systems in order to correctly close C and N budgets at regional and global scales.

Acknowledgments

This research is part of the CNP-Leyre project funded by the Cluster of Excellence COTE (LabEx COTE) at the Université de Bordeaux (ANR-10-LABX-45).

Appendix A. Supplementary data

Supplementary data to this article can be found online at <https://doi.org/10.1016/j.scitotenv.2019.01.152>.

References

- Abril, G., Borges, A.V., 2018. Carbon leaks from flooded land: do we need to re-plumb the inland water active pipe? *Biogeosci. Discuss.* 2018, 1–46. <https://doi.org/10.5194/bg-2018-239>.
- Abril, G., Martinez, J.-M., Artigas, L.F., Moreira-Turcq, P., Benedetti, M.F., Vidal, L., Meziane, T., Kim, J.-H., Bernardes, M.C., Savoye, N., Deborde, J., Souza, E.L., Albéric, P., Landim de Souza, M.F., Roland, F., 2014. Amazon River carbon dioxide outgassing fuelled by wetlands. *Nature* 505, 395–398. <https://doi.org/10.1038/nature12797>.
- Abril, G., Bouillon, S., Darchambeau, F., Teodoru, C.R., Marwick, T.R., Tamooh, F., Ochieng Omengo, F., Geeraert, N., Deirmendjian, L., Poldenaere, P., Borges, A.V., 2015. Technical note: large overestimation of pCO₂ calculated from pH and alkalinity in acidic, organic-rich freshwaters. *Biogeosciences* 12, 67–78. <https://doi.org/10.5194/bg-12-67-2015>.
- Aitkenhead, J.A., Hope, D., Billett, M.F., 1999. The relationship between dissolved organic carbon in stream water and soil organic carbon pools at different spatial scales. *Hydrol. Process.* 13, 1289–1302.
- Anderson, L., 1979. Simultaneous spectrophotometric determination of nitrite and nitrate by flow injection analysis. *Anal. Chim. Acta* 110, 123–128.
- Anderson, T.R., Groffman, P.M., Kaushal, S.S., Walter, M.T., 2014. Shallow groundwater denitrification in riparian zones of a headwater agricultural landscape. *J. Environ. Qual.* 43, 732–744.
- Asner, G.P., Elmore, A.J., Olander, L.P., Martin, R.E., Harris, A.T., 2004. Grazing systems, ecosystem responses, and global change. *Annu. Rev. Environ. Resour.* 29, 261–299.
- Augusto, L., Bakker, M.R., Morel, C., Meredieu, C., Trichet, P., Badeau, V., Arrouays, D., Plassard, C., Achat, D.L., Gallet-Budynek, A., Merzeau, D., Canteloup, D., Najar, M., Ranger, J., 2010. Is 'grey literature' a reliable source of data to characterize soils at the scale of a region? A case study in a maritime pine forest in southwestern France. *Eur. J. Soil Sci.* 61, 807–822. <https://doi.org/10.1111/j.1365-2389.2010.01286.x>.
- Baker, M.A., Dahm, C.N., Valett, H.M., 1999. Acetate retention and metabolism in the hyporheic zone of a mountain stream. *Limnol. Oceanogr.* 44, 1530–1539.
- Bakker, M.R., Augusto, L., Achat, D.L., 2006. Fine root distribution of trees and understorey in mature stands of maritime pine (*Pinus pinaster*) on dry and humid sites. *Plant Soil* 286, 37–51.
- Bakker, M.R., Jolicœur, E., Trichet, P., Augusto, L., Plassard, C., Guibert, J., Loustau, D., 2009. Adaptation of fine roots to annual fertilization and irrigation in a 13-year-old *Pinus pinaster* stand. *Tree Physiol.* 29, 229–238.
- Balestrini, R., Sacchi, E., Tidili, D., Delconte, C.A., Buffagni, A., 2016. Factors affecting agricultural nitrogen removal in riparian strips: examples from groundwater-dependent ecosystems of the Po Valley (Northern Italy). *Agric. Ecosyst. Environ.* 221, 132–144.
- Bardini, L., Boano, F., Cardenas, M.B., Revelli, R., Rodolfi, L., 2012. Nutrient cycling in bedform induced hyporheic zones. *Geochim. Cosmochim. Acta* 84, 47–61.
- Barnes, R.T., Raymond, P.A., 2009. The contribution of agricultural and urban activities to inorganic carbon fluxes within temperate watersheds. *Chem. Geol.* 266, 318–327.
- Barnes, R.T., Raymond, P.A., 2010. Land-use controls on sources and processing of nitrate in small watersheds: insights from dual isotopic analysis. *Ecol. Appl.* 20, 1961–1978.
- Bass, A.M., Munksgaard, N.C., Leblanc, M., Tweed, S., Bird, M.J., 2014. Contrasting carbon export dynamics of human impacted and pristine tropical catchments in response to a short-lived discharge event. *Hydrol. Process.* 28, 1835–1843.
- Bastviken, D., Tranvik, L.J., Downing, J.A., Crill, P.M., Enrich-Prast, A., 2011. Freshwater methane emissions offset the continental carbon sink. *Science* 331 (50–50).
- Bell, R.A., Darling, W.G., Ward, R.S., Basava-Reddi, L., Halwa, L., Manamsa, K., Dochartaigh, B.O., 2017. A baseline survey of dissolved methane in aquifers of Great Britain. *Sci. Total Environ.* 601, 1803–1813.
- Bernot, M.J., Sobota, D.J., Hall, R.O., Mulholland, P.J., Dodds, W.K., Webster, J.R., Tank, J.L., Ashkenas, L.R., Cooper, L.W., Dahm, C.N., 2010. Inter-regional comparison of land-use effects on stream metabolism. *Freshw. Biol.* 55, 1874–1890.
- Bertran, P., Alletet, G., Gé, T., Naughton, F., Poirier, P., Goñi, M.F.S., 2009. Coversand and Pleistocene palaeosols in the Landes region, southwestern France. *J. Quat. Sci.* 24, 259–269.
- Bertran, P., Bateman, M.D., Hernandez, M., Mercier, N., Millet, D., Sizia, L., Tastet, J.-P., 2011. Inland aeolian deposits of south-West France: facies, stratigraphy and chronology. *J. Quat. Sci.* 26, 374–388.
- Bodmer, P., Heinz, M., Pusch, M., Singer, G., Premke, K., 2016. Carbon dynamics and their link to dissolved organic matter quality across contrasting stream ecosystems. *Sci. Total Environ.* 553, 574–586.
- Böhlke, J.K., Antweiler, R.C., Harvey, J.W., Laursen, A.E., Smith, L.K., Smith, R.L., Voytek, M.A., 2009. Multi-scale measurements and modeling of denitrification in streams with varying flow and nitrate concentration in the upper Mississippi River basin, USA. *Biogeochemistry* 93, 117–141.
- Borges, A.V., Darchambeau, F., Teodoru, C.R., Marwick, T.R., Tamooh, F., Geeraert, N., Omengo, F.O., Guérin, F., Lambert, T., Morana, C., Okuku, E., Bouillon, S., 2015. Globally significant greenhouse-gas emissions from African inland waters. *Nat. Geosci.* 8, 637–642. <https://doi.org/10.1038/ngeo2486>.
- Borges, A.V., Darchambeau, F., Lambert, T., Bouillon, S., Morana, C., Brouyère, S., Hakoun, V., Jurado, A., Tseng, H.-C., Descy, J.-P., 2018. Effects of agricultural land use on fluvial carbon dioxide, methane and nitrous oxide concentrations in a large European river, the Meuse (Belgium). *Sci. Total Environ.* 610, 342–355.
- Camino-Serrano, M., Gielen, B., Luysaert, S., Ciais, P., Vicca, S., Guenet, B., Vos, B.D., Cools, N., Ahrens, B., Altaf Arain, M., Borken, W., Clarke, N., Clarkson, B., Cummins, T., Don, A., Graf Pannatier, E., Laudon, H., Moore, T., Nieminen, T., Nilsson, M.B., Peichi, M., Schwendenmann, L., Siemens, J., Janssens, I.A., 2014. Linking variability in soil solution dissolved organic carbon to climate, soil type, and vegetation type. *Glob. Biogeochem. Cycles* 28, 497–509. <https://doi.org/10.1002/2013GB004726>.
- Canton, M., Anschutz, P., Coynel, A., Poldenaere, P., Aubry, I., Poirier, D., 2012. Nutrient export to an Eastern Atlantic coastal zone: first modeling and nitrogen mass balance. *Biogeochemistry* 107, 361–377.
- Carpenter, S.R., Caraco, N.F., Correll, D.L., Howarth, R.W., Sharpley, A.N., Smith, V.H., 1998. Nonpoint pollution of surface waters with phosphorus and nitrogen. *Ecol. Appl.* 8, 559–568.
- Cey, E.E., Rudolph, D.L., Aravena, R., Parkin, G., 1999. Role of the riparian zone in controlling the distribution and fate of agricultural nitrogen near a small stream in southern Ontario. *J. Contam. Hydrol.* 37, 45–67.
- Christensen, T.R., Ekberg, A., Ström, L., Mastepanov, M., Panikov, N., Öquist, M., Svensson, B.H., Nykänen, H., Martikainen, P.J., Oskarsson, H., 2003. Factors controlling large scale variations in methane emissions from wetlands. *Geophys. Res. Lett.* 30.
- Christensen, J.R., Nash, M.S., Neale, A., 2013. Identifying riparian buffer effects on stream nitrogen in southeastern coastal plain watersheds. *Environ. Manag.* 52, 1161–1176.
- Ciais, P., Wattenbach, M., Vuichard, N., Smith, P., Piao, S.L., Don, A., Luysaert, S., Janssens, I.A., Bondeau, A., Dechow, R., et al., 2010. The European carbon balance. Part 2: croplands. *Glob. Chang. Biol.* 16, 1409–1428.
- Clague, J.C., Stenger, R., Clough, T.J., 2015. Denitrification in the shallow groundwater system of a lowland catchment: a laboratory study. *Catena* 131, 109–118.
- Clark, I., Fritz, P., 1997. *Environmental Isotopes in Hydrology*. Lewis Publishers, Boca Raton, Fla.
- Cole, J.J., Prairie, Y.T., Caraco, N.F., McDowell, W.H., Tranvik, L.J., Striegl, R.G., Duarte, C.M., Kortelainen, P., Downing, J.A., Middelburg, J.J., Melack, J., 2007. Plumbing the global carbon cycle: integrating inland waters into the terrestrial carbon budget. *Ecosystems* 10, 171–184. <https://doi.org/10.1007/s10021-006-9013-8>.
- Corbier, P., Karnay, G., Bourguin, B., Saltel, M., 2010. Gestion des eaux souterraines en région Aquitaine - Reconnaissance des potentialités aquifères du Mio-Plio-Quaternaire des kandes de Gascogne et du Médoc en relation avec les SAGE, Module 7 (No. 57813). BRGM, Orléans, France.
- Cotton, J.A., Wharton, G., Bass, J.A.B., Heppell, C.M., Wotton, R.S., 2006. The effects of seasonal changes to in-stream vegetation cover on patterns of flow and accumulation of sediment. *Geomorphology* 77, 320–334.
- Crawford, J.T., Loken, L.C., Stanley, E.H., Stets, E.G., Dornblaser, M.M., Striegl, R.G., 2016. Basin scale controls on CO₂ and CH₄ emissions from the Upper Mississippi River. *Geophys. Res. Lett.* 43, 1973–1979.
- Das, A., Krishnaswami, S., Bhattacharya, S.K., 2005. Carbon isotope ratio of dissolved inorganic carbon (DIC) in rivers draining the Deccan traps, India: sources of DIC and their magnitudes. *Earth Planet. Sci. Lett.* 236, 419–429.
- Datry, T., Malard, F., Gibert, J., 2004. Dynamics of solutes and dissolved oxygen in shallow urban groundwater below a stormwater infiltration basin. *Sci. Total Environ.* 329, 215–229.
- De Carvalho, M.C., Hayashizaki, K.-I., Ogawa, H., 2009. Short-term measurement of carbon stable isotope discrimination in photosynthesis and respiration by aquatic macrophytes, with marine macroalgal examples 1. *J. Phycol.* 45, 761–770.
- De Wit, R., Leibreich, J., Vernier, F., Delmas, F., Beuffe, H., Maison, P., Chossat, J.-C., Laplace-Treytoure, C., Laplana, R., Clave, V., 2005. Relationship between land-use in the agroforestry system of les Landes, nitrogen loading to and risk of macro-algal blooming in the Bassin d'Arcachon coastal lagoon (SW France). *Estuar. Coast. Shelf Sci.* 62, 453–465.
- Deirmendjian, L., Abril, G., 2018. Carbon dioxide degassing at the groundwater-stream-atmosphere interface: isotopic equilibration and hydrological mass balance in a sandy watershed. *J. Hydrol.* 558, 129–143. <https://doi.org/10.1016/j.jhydrol.2018.01.003>.
- Deirmendjian, L., Loustau, D., Augusto, L., Lafont, S., Chipeaux, C., Poirier, D., Abril, G., 2018. Hydro-ecological controls on dissolved carbon dynamics in groundwater and export to streams in a temperate pine forest. *Biogeosciences* 15, 669–691. <https://doi.org/10.5194/bg-15-669-2018>.
- Downing, J.A., Cole, J.J., Duarte, C.M., Middelburg, J.J., Melack, J.M., Prairie, Y.T., Kortelainen, P., Striegl, R.G., McDowell, W.H., Tranvik, L.J., 2012. Global abundance and size distribution of streams and rivers. *Inland Waters* 2, 229–236.
- EEA, 2014. European Environmental Agency, Corine Land Cover 2006 raster data. Retrieved from <http://www.eea.europa.eu/data-and-maps/data/corine-land-cover-2006-raster-3>.

- Etcheber, H., Taillez, A., Abril, G., Garnier, J., Servais, P., Moatar, F., Commarieu, M.-V., 2007. Particulate organic carbon in the estuarine turbidity maxima of the Gironde, Loire and Seine estuaries: origin and lability. *Hydrobiologia* 588, 245–259.
- Evans, S.D., Lindstrom, M.J., Voorhees, W.B., Moncrief, J.F., Nelson, G.A., 1996. Effect of subsoiling and subsequent tillage on soil bulk density, soil moisture, and corn yield. *Soil Tillage Res.* 38, 35–46.
- Findlay, S., 1995. Importance of surface-subsurface exchange in stream ecosystems: the hyporheic zone. *Limnol. Oceanogr.* 40, 159–164.
- Findlay, S., Quinn, J.M., Hickey, C.W., Burrell, G., Downes, M., 2001. Effects of land use and riparian flowpath on delivery of dissolved organic carbon to streams. *Limnol. Oceanogr.* 46, 345–355.
- Foley, J.A., DeFries, R., Asner, G.P., Barford, C., Bonan, G., Carpenter, S.R., Chapin, F.S., Coe, M.T., Daily, G.C., Gibbs, H.K., 2005. Global consequences of land use. *Science* 309, 570–574.
- Foulquier, A., Malard, F., Mermillod-Blondin, F., Detry, T., Simon, L., Montuelle, B., Gibert, J., 2010. Vertical change in dissolved organic carbon and oxygen at the water table region of an aquifer recharged with stormwater: biological uptake or mixing? *Biogeochemistry* 99, 31–47.
- Frankignoulle, M., Borges, A.V., 2001. Direct and indirect pCO₂ measurements in a wide range of pCO₂ and salinity values (the Scheldt estuary). *Aquat. Geochem.* 7, 267–273. <https://doi.org/10.1023/A:1015251010481>.
- Fuss, T., Behounek, B., Ulseth, A.J., Singer, G.A., 2017. Land use controls stream ecosystem metabolism by shifting dissolved organic matter and nutrient regimes. *Freshw. Biol.* 62, 582–599.
- Gillikin, D.P., Bouillon, S., 2007. Determination of $\delta^{18}O$ of water and $\delta^{13}C$ of dissolved inorganic carbon using a simple modification of an elemental analyser-isotope ratio mass spectrometer: an evaluation. *Rapid Commun. Mass Spectrom.* 21, 1475–1478.
- Gleick, P.H., 2003. Water use. *Annu. Rev. Environ. Resour.* 28, 275–314.
- Goldscheider, N., Hunkeler, D., Rossi, P., 2006. Microbial biocenoses in pristine aquifers and an assessment of investigative methods. *Hydrogeol. J.* 14, 926–941.
- Govind, A., Bonnefond, J.-M., Kumari, J., Moisy, C., Loustau, D., Wigneron, J.-P., 2012. Modeling the ecohydrological processes in the Landes de Gascogne, SW France, in: plant growth modeling, simulation, visualization and applications (PMA). 2012 IEEE Fourth International Symposium On. IEEE, pp. 133–140.
- Graeber, D., Boëchat, I.G., Encina-Montoya, F., Esse, C., Gelbrecht, J., Goyenola, G., Gücker, B., Heinz, M., Kronvang, B., Meerhoff, M., 2015. Global effects of agriculture on fluvial dissolved organic matter. *Sci. Rep.* 5.
- Gran, G., 1952. Determination of the equivalence point in potentiometric titrations of seawater with hydrochloric acid. *Oceanol. Acta* 5, 209–218.
- Hagedorn, F., Kaiser, K., Feyen, H., Schleppl, P., 2000. Effects of redox conditions and flow processes on the mobility of dissolved organic carbon and nitrogen in a forest soil. *J. Environ. Qual.* 29, 288–297.
- Hagerdon, F., Schleppl, P., Waldner, P., Fluhler, H., 2000. Export of dissolved organic carbon and nitrogen from Gleysol dominated catchments—the significance of water flow paths. *Biogeochemistry* 50, 137–161.
- Harwood, J.E., Kühn, A.L., 1970. A colorimetric method for ammonia in natural waters. *Water Res.* 4, 805–811. [https://doi.org/10.1016/0043-1354\(70\)90037-0](https://doi.org/10.1016/0043-1354(70)90037-0).
- Hiscock, K.M., Lloyd, J.W., Lerner, D.N., 1991. Review of natural and artificial denitrification of groundwater. *Water Res.* 25, 1099–1111.
- Hotchkiss, E.R., Hall Jr, R.O., Sponseller, R.A., Butman, D., Klaminder, J., Laudon, H., Rosvall, M., Karlsson, J., 2015. Sources of and processes controlling CO₂ emissions change with the size of streams and rivers. *Nat. Geosci.* 8, 696–699.
- Hu, Y., Lu, Y., Edmonds, J.W., Liu, C., Wang, S., Das, O., Liu, J., Zheng, C., 2016. Hydrological and land use control of watershed exports of dissolved organic matter in a large arid river basin in northwestern China. *J. Geophys. Res. Biogeosci.* 121, 466–478.
- Jackson, R.B., Carpenter, S.R., Dahm, C.N., McKnight, D.M., Naiman, R.J., Postel, S.L., Running, S.W., 2001. Water in a changing world. *Ecol. Appl.* 11, 1027–1045.
- Jambert, C., Delmas, R.A., Labroue, L., Chassin, P., 1994. Nitrogen compound emissions from fertilized soils in a maize field pine tree forest agrosystem in the southwest of France. *J. Geophys. Res.-Atmos.* 99, 16523–16530.
- Jambert, C., Serca, D., Delmas, R., 1997. Quantification of N-losses as NH₃, NO, and N₂O and N₂ from fertilized maize fields in southwestern France. *Nutr. Cycl. Agroecosyst.* 48, 91–104.
- Jeong, C.H., 2001. Effect of land use and urbanization on hydrochemistry and contamination of groundwater from Taejon area, Korea. *J. Hydrol.* 253, 194–210.
- Johnson, M.S., Lehmann, J., Couto, E.G., Novaes Filho, J.P., Riha, S.J., 2006. DOC and DIC in flowpaths of Amazonian headwater catchments with hydrologically contrasting soils. *Biogeochemistry* 81, 45–57.
- Johnson, M.S., Lehmann, J., Riha, S.J., Krusche, A.V., Richey, J.E., Ometto, J.P.H., Couto, E.G., 2008. CO₂ efflux from Amazonian headwater streams represents a significant fate for deep soil respiration. *Geophys. Res. Lett.* 35, L17401. <https://doi.org/10.1029/2008GL034619>.
- Jolivet, C., Arrouays, D., Andreux, F., Lévêque, J., 1997. Soil organic carbon dynamics in cleared temperate forest spodosols converted to maize cropping. *Plant Soil* 191, 225–231.
- Jolivet, C., Arrouays, D., Leveque, J., Andreux, F., Chenu, C., 2003. Organic carbon dynamics in soil particle-size separates of sandy Spodosols when forest is cleared for maize cropping. *Eur. J. Soil Sci.* 54, 257–268.
- Jolivet, C., Augusto, L., Trichet, P., Arrouays, D., 2007. Forest soils in the Gascony Landes region: formation, history, properties and spatial variability. *Rev. For.* 59, 7–30. <https://doi.org/10.4267/2042/8480>.
- Jones, J.B., Mulholland, P.J., 1998. Carbon dioxide variation in a hardwood forest stream: an integrative measure of whole catchment soil respiration. *Ecosystems* 1, 183–196.
- Jordan, T.E., Weller, D.E., 1996. Human contributions to terrestrial nitrogen flux. *Bioscience* 46, 655–664.
- Jurado, A., Borges, A., Pujades, E., Hakoun, V., Knöller, K., Brouyère, S., 2017. Occurrence of greenhouse gases (CO₂, N₂O and CH₄) in groundwater of the Walloon Region (Belgium). *Tauzin, J., Dureau, P., Courpron, C., 1982. Exportation des éléments fertilisants par lessivage en sol sableux des Landes de Gascogne. Résultats de 8 années d'observations en cases lysimétriques. Agronomie* 2, 91–98.
- Kankaala, P., Käkki, T., Mäkelä, S., Ojala, A., Pajunen, H., Arvola, L., 2005. Methane efflux in relation to plant biomass and sediment characteristics in stands of three common emergent macrophytes in boreal mesoeutrophic lakes. *Glob. Chang. Biol.* 11, 145–153.
- Kassambara, A., Mundt, F., 2017. factoextra: Extract and Visualize the Results of Multivariate Data Analyses. R Package Version 1.0.e5.
- Klüber, H.D., Conrad, R., 1998. Effects of nitrate, nitrite, NO and N₂O on methanogenesis and other redox processes in anoxic rice field soil. *FEMS Microbiol. Ecol.* 25, 301–318.
- Kokic, J., Wallin, M.B., Chmiel, H.E., Denfeld, B.A., Sobek, S., 2015. Carbon dioxide evasion from headwater systems strongly contributes to the total export of carbon from a small boreal lake catchment. *J. Geophys. Res. Biogeosci.* 120, 13–28. <https://doi.org/10.1002/2014JG002706>.
- Kolbjørn Jensen, J., Engesgaard, P., Johnsen, A.R., Marti, V., Nilsson, B., 2017. Hydrological mediated denitrification in groundwater below a seasonal flooded restored riparian zone. *Water Resour. Res.* 53, 2074–2094.
- Korom, S.F., 1992. Natural denitrification in the saturated zone: a review. *Water Resour. Res.* 28, 1657–1668.
- Lamba, J., Thompson, A.M., Karthikeyan, K., Fitzpatrick, F.A., 2015. Sources of fine sediment stored in agricultural lowland streams, Midwest, USA. *Geomorphology* 236, 44–53.
- Lauerwald, R., Laruelle, G.G., Hartmann, J., Ciais, P., Regnier, P.A., 2015. Spatial patterns in CO₂ evasion from the global river network. *Glob. Biogeochem. Cycles* 29, 534–554.
- Lê, S., Josse, J., Husson, F., 2008. FactoMineR: an R package for multivariate analysis. *J. Stat. Softw.* 25, 1–18.
- Legigán, P., 1979. L'élaboration de la formation du sable des Landes, dépôt résiduel de l'environnement sédimentaire pliocène-pléistocène centre aquitain (Thèse de Doctorat d'Etat n°642). Université de Bordeaux I, Bordeaux.
- Lehrter, J.C., 2006. Effects of land use and land cover, stream discharge, and interannual climate on the magnitude and timing of nitrogen, phosphorus, and organic carbon concentrations in three coastal plain watersheds. *Water Environ. Res.* 78, 2356–2368.
- Lewis, E., Wallace, D., Allison, L.J., 1998. Program Developed for CO₂ System Calculations. Carbon Dioxide Information Analysis Center, Oak Ridge, Tennessee managed by Lockheed Martin Energy Research Corporation for the US Department of Energy Tennessee.
- Lewis, M.A., Weber, D.E., Stanley, R.S., Moore, J.C., 2001. Dredging impact on an urbanized Florida bayou: effects on benthos and algal-periphyton. *Environ. Pollut.* 115, 161–171.
- Ludwig, W., Amiotte-Suchet, P., Probst, J.-L., 1996a. River discharges of carbon to the world's oceans: determining local inputs of alkalinity and of dissolved and particulate organic carbon. *Sci. Terre Planètes Comptes Rendus Académie Sci.* 323, 1007–1014.
- Ludwig, W., Probst, J.-L., Kempe, S., 1996b. Predicting the oceanic input of organic carbon by continental erosion. *Glob. Biogeochem. Cycles* 10, 23–41.
- Lundström, U.S., van Breemen, N., Bain, D., 2000. The podzolization process. A review. *Geoderma* 94, 91–107.
- MacQueen, J., 1967. Some methods for classification and analysis of multivariate observations. *Proceedings of the Fifth Berkeley Symposium on Mathematical Statistics and Probability*. Oakland, CA, USA, pp. 281–297.
- Malard, F., Hervant, F., 1999. Oxygen supply and the adaptations of animals in groundwater. *Freshw. Biol.* 41, 1–30.
- Marx, A., Dusek, J., Jankovec, J., Sanda, M., Vogel, T., van Geldern, R., et al., 2017. A review of CO₂ and associated carbon dynamics in headwater streams: a global perspective. *Rev. Geophys.* 55 (2), 560–585. <https://doi.org/10.1002/2016RG000547>.
- Masese, F.O., Salcedo-Borda, J.S., Gettel, G.M., Irvine, K., McClain, M.E., 2017. Influence of catchment land use and seasonality on dissolved organic matter composition and ecosystem metabolism in headwater streams of a Kenyan river. *Biogeochemistry* 132, 1–22.
- McAleer, E.B., Coxon, C.E., Richards, K.G., Jahangir, M.M.R., Grant, J., Mellander, P.E., 2017. Groundwater nitrate reduction versus dissolved gas production: a tale of two catchments. *Sci. Total Environ.* 586, 372–389.
- McClain, M.E., Boyer, E.W., Dent, C.L., Gergel, S.E., Grimm, N.B., Groffman, P.M., Hart, S.C., Harvey, J.W., Johnston, C.A., Mayorga, E., McDowell, W.H., Pinay, G., 2003. Biogeochemical hot spots and hot moments at the interface of terrestrial and aquatic ecosystems. *Ecosystems* 6, 301–312.
- McMahon, P.B., Chapelle, F.H., 2008. Redox processes and water quality of selected principal aquifer systems. *Groundwater* 46, 259–271.
- Mekala, C., Gaonkar, O., Nambi, I.M., 2017. Understanding nitrogen and carbon biogeochemical transformations and transport dynamics in saturated soil columns. *Geoderma* 285, 185–194.
- Meybeck, M., 1982. Carbon, nitrogen, and phosphorus transport by world rivers. *Am. J. Sci.* 282, 401–450.
- Meybeck, M., 1987. Global chemical weathering of surficial rocks estimated from river dissolved loads. *Am. J. Sci.* 401–428.
- Millero, F.J., 1979. The thermodynamics of the carbonate system in seawater. *Geochim. Cosmochim. Acta* 43, 1651–1661.
- Molofsky, L.J., Connor, J.A., McHugh, T.E., Richardson, S.D., Woroszylow, C., Alvarez, P.J., 2016. Environmental factors associated with natural methane occurrence in the Appalachian Basin. *Groundwater* 54, 656–668.
- Montgomery, D.R., 2007. Soil erosion and agricultural sustainability. *Proc. Natl. Acad. Sci.* 104, 13268–13272.

- Moore, T.R., Knowles, R., 1989. The influence of water table levels on methane and carbon dioxide emissions from peatland soils. *Can. J. Soil Sci.* 69, 33–38.
- Moreaux, V., Lamaud, É., Bosc, A., Bonnefond, J.-M., Medlyn, B.E., Loustau, D., 2011. Paired comparison of water, energy and carbon exchanges over two young maritime pine stands (*Pinus pinaster* Ait.): effects of thinning and weeding in the early stage of tree growth. *Tree Physiol.*, 903–921 <https://doi.org/10.1093/treephys/tpr048>.
- Morrice, J.A., Valett, H.M., Dahm, C.N., Campana, M.E., 1997. Alluvial characteristics, groundwater–surface water exchange and hydrological retention in headwater streams. *Hydrol. Process.* 11, 253–267.
- Mulholland, P.J., Tank, J.L., Sanzone, D.M., Wollheim, W.M., Peterson, B.J., Webster, J.R., Meyer, J.L., 2000. Nitrogen cycling in a forest stream determined by a ¹⁵N tracer addition. *Ecol. Monogr.* 70, 471–493.
- Mulholland, P.J., Helton, A.M., Poole, G.C., Hall, R.O., Hamilton, S.K., Peterson, B.J., Tank, J.L., Ashkenas, L.R., Cooper, L.W., Dahm, C.N., 2008. Stream denitrification across biomes and its response to anthropogenic nitrate loading. *Nature* 452, 202.
- Naumburg, E., Mata-Gonzalez, R., Hunter, R.G., McIendon, T., Martin, D.W., 2005. Phreatophytic vegetation and groundwater fluctuations: a review of current research and application of ecosystem response modeling with an emphasis on Great Basin vegetation. *Environ. Manag.* 35, 726–740.
- Newell, R.C., Seiderer, L.J., Hitchcock, D.R., 1998. The impact of dredging works in coastal waters: a review of the sensitivity to disturbance and subsequent recovery of biological resources on the sea bed. *Oceanogr. Mar. Biol. Annu. Rev.* 36, 127–178.
- O'Leary, M.H., 1988. Carbon isotopes in photosynthesis. *Bioscience* 328–336.
- Onderka, M., Pekarova, P., Miklanek, P., Halmova, D., Pekar, J., 2010. Examination of the dissolved inorganic nitrogen budget in three experimental microbasins with contrasting land cover—a mass balance approach. *Water Air Soil Pollut.* 210, 221–230.
- O'Reilly, A.M., Chang, N.-B., Waniellista, M.P., 2012. Cyclic biogeochemical processes and nitrogen fate beneath a subtropical stormwater infiltration basin. *J. Contam. Hydrol.* 133, 53–75.
- Otero, N., Torrentó, C., Soler, A., Menció, A., Mas-Pla, J., 2009. Monitoring groundwater nitrate attenuation in a regional system coupling hydrogeology with multi-isotopic methods: the case of Plana de Vic (Osona, Spain). *Agric. Ecosyst. Environ.* 133, 103–113.
- Pabich, W.J., Valiela, I., Hemond, H.F., 2001. Relationship between DOC concentration and vadose zone thickness and depth below water table in groundwater of Cape Cod, USA. *Biogeochemistry* 55, 247–268.
- Polsenaere, P., Abril, G., 2012. Modelling CO₂ degassing from small acidic rivers using water pCO₂, DIC and δ¹³C-DIC data. *Geochim. Cosmochim. Acta* 91, 220–239. <https://doi.org/10.1016/j.gca.2012.05.030>.
- Polsenaere, P., Savoye, N., Etcheber, H., Canton, M., Poirier, D., Bouillon, S., Abril, G., 2013. Export and degassing of terrestrial carbon through watercourses draining a temperate podzolized catchment. *Aquat. Sci.* 75, 299–319.
- Postel, S., 1999. Pillar of Sand: Can the Irrigation Miracle Last? WW Norton & Company.
- Quéné, K., Derenne, S., Largeau, C., Rumpel, C., Mariotti, A., 2006. Influence of change in land use on the refractory organic macromolecular fraction of a sandy spodosol (Landes de Gascogne, France). *Geoderma* 136, 136–151.
- Quinton, J.N., Govers, G., Van Oost, K., Bardgett, R.D., 2010. The impact of agricultural soil erosion on biogeochemical cycling. *Nat. Geosci.* 3, 311–314.
- R Core Team, 2018. R: A Language and Environment for Statistical Computing. R Foundation for Statistical Computing, Vienna, Austria.
- Ramankutty, N., Foley, J.A., 1999. Estimating historical changes in global land cover: croplands from 1700 to 1992. *Glob. Biogeochem. Cycles* 13, 997–1027.
- Ramos, T.B., Rodrigues, S., Branco, M.A., Prazeres, A., Brito, D., Gonçalves, M.C., Martins, J.C., Fernandes, M.L., Pires, F.P., 2015. Temporal variability of soil organic carbon transport in the Enxôe agricultural watershed. *Environ. Earth Sci.* 73, 6663–6676.
- Raven, J.A., Johnston, A.M., Kübler, J.E., Korb, R., McInroy, S.G., Handley, L.L., Scrimgeour, C.M., Walker, D.I., Beardall, J., Vanderklift, M., 2002. Mechanistic interpretation of carbon isotope discrimination by marine macroalgae and seagrasses. *Funct. Plant Biol.* 29, 355–378.
- Ravishankara, A.R., Daniel, J.S., Portmann, R.W., 2009. Nitrous oxide (N₂O): the dominant ozone-depleting substance emitted in the 21st century. *Science* 326, 123–125.
- Raymond, P.A., Cole, J.J., 2003. Increase in the export of alkalinity from North America's largest river. *Science* 301, 88–91.
- Raymond, P.A., Hartmann, J., Lauerwald, R., Sobek, S., McDonald, C., Hoover, M., Butman, D., Striegl, R., Mayorga, E., Humborg, C., Kortelainen, P., Dürr, H., Meybeck, M., Ciais, P., Guth, P., 2013. Global carbon dioxide emissions from inland waters. *Nature* 503, 355–359. <https://doi.org/10.1038/nature12760>.
- Rimmel, P., 1998. Etude des apports allochtones d'azote inorganique dissous parvenant à un système lagunaire: le Bassin d'Arcachon.
- Robinson, M., Ryder, E.L., Ward, R.C., 1985. Influence on streamflow of field drainage in a small agricultural catchment. *Agric. Water Manag.* 10, 145–158.
- Rodrigues, V., Estrany, J., Ranzini, M., de Cicco, V., Martín-Benito, J.M.T., Hedo, J., Lucas-Borja, M.E., 2018. Effects of land use and seasonality on stream water quality in a small tropical catchment: the headwater of Córrego Água Limpá, São Paulo (Brazil). *Sci. Total Environ.* 622, 1553–1561.
- Rosegrant, M.W., Cai, X., Cline, S.A., 2002. World Water and Food to 2025: Dealing with Scarcity. Intl Food Policy Res Inst.
- Rubol, S., Silver, W.L., Bellin, A., 2012. Hydrologic control on redox and nitrogen dynamics in a peatland soil. *Sci. Total Environ.* 432, 37–46.
- Rubol, S., Dutta, T., Rocchini, D., 2016. 2D visualization captures the local heterogeneity of oxidative metabolism across soils from diverse land-use. *Sci. Total Environ.* 572, 713–723.
- Salomons, W., Mook, W.G., 1986. Isotope geochemistry of carbonates in the weathering zone. *Handb. Environ. Isot. Geochem.* 2, pp. 239–269.
- Salvia-Castellví, M., Iffly, J.F., Vander Borgh, P., Hoffmann, L., 2005. Dissolved and particulate nutrient export from rural catchments: a case study from Luxembourg. *Sci. Total Environ.* 344, 51–65.
- Sanders, I.A., Heppell, C.M., Cotton, J.A., Wharton, G., Hildrew, A.G., Flowers, E.J., Trimmer, M., 2007. Emission of methane from chalk streams has potential implications for agricultural practices. *Freshw. Biol.* 52, 1176–1186.
- Sand-Jensen, K., Pedersen, O., 1999. Velocity gradients and turbulence around macrophyte stands in streams. *Freshw. Biol.* 42, 315–328.
- Schade, J.D., Bailio, J., McDowell, W.H., 2016. Greenhouse gas flux from headwater streams in New Hampshire, USA: patterns and drivers. *Limnol. Oceanogr.* 61.
- Sharp, J.H., 1993. The dissolved organic carbon controversy: an update. *Oceanography* 6.
- Silver, W.L., Lugo, A.E., Keller, M., 1999. Soil oxygen availability and biogeochemistry along rainfall and topographic gradients in upland wet tropical forest soils. *Biogeochemistry* 44, 301–328.
- Smith, V.H., 2003. Eutrophication of freshwater and coastal marine ecosystems a global problem. *Environ. Sci. Pollut. Res.* 10, 126–139.
- Stanley, E.H., Casson, N.J., Christel, S.T., Crawford, J.T., Loken, L.C., Oliver, S.K., 2016. The ecology of methane in streams and rivers: patterns, controls, and global significance. *Ecol. Monogr.* 86, 146–171.
- Starr, R.C., Gillham, R.W., 1993. Denitrification and organic carbon availability in two aquifers. *Groundwater* 31, 934–947.
- Stella, P., Lamaud, E., Brunet, Y., Bonnefond, J.-M., Loustau, D., Irvine, M., 2009. Simultaneous measurements of CO₂ and water exchanges over three agroecosystems in South-West France. *Biogeosciences* 6, 2957–2971.
- Stookey, L.L., 1970. Ferrozine—a new spectrophotometric reagent for iron. *Anal. Chem.* 42, 779–781.
- Stott, T., 2005. Natural recovery from accelerated forest ditch and stream bank erosion five years after harvesting of plantation forest on Plynlimon, mid-Wales. *Earth Surf. Process. Landf. J. Br. Geomorphol. Res. Group* 30, 349–357.
- Thivolle-Cazat, A., Najar, M., 2001. Évolution de la productivité et de la récolte du pin maritime dans le massif Landais. Evaluation de la disponibilité future en Gironde. *Rev. For. Fr.* 53, 351–355.
- Trichet, P., Bakker, M.R., Augusto, L., Alazard, P., Merzeau, D., Saur, E., 2009. Fifty years of fertilization experiments on *Pinus pinaster* in Southwest France: the importance of phosphorus as a fertilizer. *For. Sci.* 55, 390–402.
- Tsypin, M., Macpherson, G.L., 2012. The effect of precipitation events on inorganic carbon in soil and shallow groundwater, Konza Prairie LTER Site, NE Kansas, USA. *Appl. Geochem.* 27, 2356–2369.
- Ulrich, E., Coddeville, P., Lanier, M., 2002. Retombées atmosphériques humides en France entre 1993 et 1998: [données et références-coordination technique de la surveillance de la qualité de l'air]. Ademe.
- Vernier, F., Castro, A., 2010. Critère Préservation de l'environnement Sous-critère Eau (Rapport d'expertise: Critère "Préservation de l'environnement"). GIP-ECOFOR. Bordeaux, France.
- Vernier, F., Beuffe, H., Chossat, J.-C., 2003. Forêt et ressource en eau: étude de deux bassins versants en sol sableux (Landes de Gascogne). *Rev. For. Fr.* 55, 523–542.
- Vidon, P., Wagner, L.E., Soyeux, E., 2008. Changes in the character of DOC in streams during storms in two Midwestern watersheds with contrasting land uses. *Biogeochemistry* 88, 257–270.
- Vogel, J.C., Ehleringer, J.R., Hall, A.E., Farquhar, G.D., 1993. Variability of carbon isotope fractionation during photosynthesis. *Stable Isotopes and Plant Carbon-Water Relations*. Academic Press Inc., pp. 29–46.
- Wachniew, P., 2006. Isotopic composition of dissolved inorganic carbon in a large polluted river: the Vistula, Poland. *Chem. Geol.* 233, 293–308.
- Wallin, M.B., Grabs, T., Buffam, I., Laudon, H., Ågren, A., Öquist, M.G., Bishop, K., 2013. Evasion of CO₂ from streams – the dominant component of the carbon export through the aquatic conduit in a boreal landscape. *Glob. Chang. Biol.* 19, 785–797. <https://doi.org/10.1111/gcb.12083>.
- Weiss, R., 1974. Carbon dioxide in water and seawater: the solubility of a non-ideal gas. *Mar. Chem.* 2, 203–215.
- Widdel, F., Schnell, S., Heising, S., Ehrenreich, A., Assmus, B., Schink, B., 1993. Ferrous iron oxidation by anoxygenic phototrophic bacteria. *Nature* 362, 834.
- Wilson, H.F., Xenopoulos, M.A., 2009. Effects of agricultural land use on the composition of fluvial dissolved organic matter. *Nat. Geosci.* 2, 37–41.
- Wynn, T.M., Mostaghimi, S., 2006. Effects of riparian vegetation on stream bank subaerial processes in southwestern Virginia, USA. *Earth Surf. Process. Landf.* 31, 399–413. *J. Br. Geomorphol. Res. Group*.
- Young, R.C., Huryn, A.D., 1999. Effects of land use on stream metabolism and organic matter turnover. *Ecol. Appl.* 9, 1359–1376.
- Zhang, F., Wang, J., Wang, X., 2018. Recognizing the relationship between spatial patterns in water quality and land-use/cover types: a case study of the Jinghe Oasis in Xinjiang, China. *Water* 10, 646.
- Zhou, Y., Xu, J.F., Yin, W., Ai, L., Fang, N.F., Tan, W.F., Yan, F.L., Shi, Z.H., 2017. Hydrological and environmental controls of the stream nitrate concentration and flux in a small agricultural watershed. *J. Hydrol.* 545, 355–366.